CHAPTER 5

Synthesis, Structural Analysis, and Gas-Phase Studies of 2-Quinuclidonium Tetrafluoroborate[†]

5.1 INTRODUCTION AND BACKGROUND

5.1.1 THE AMIDE LINKAGE

The amide bond is one of the most fundamental motifs in biology and chemistry as it plays the essential role of linking functionality between amino acids in peptides. Extensive studies over the past century have delineated the unique properties of this indispensable functional group.[1] Typical amides exhibit remarkable stability, with half-lives in aqueous solution exceeding hundreds of years.[2] This stability is in part due to resonance stabilization between the π-orbitals of the O–C–N linkage (Figure 5.1.1).[1,3] The significant contribution of this resonance structure also gives rise to a planar

---

[†] This work was performed in collaboration with Tony Ly, a graduate student in laboratory of Prof. Ryan Julian at the University of California, Riverside, Don K. Pham, a summer NSF REU fellow in the Julian group, Dr. Kousuke Tani, a postdoctoral scholar in the Stoltz group, and Dr. Ryan R. Julian, assistant Prof. of Chemistry at the University of California, Riverside. These works have been published. See: (a) Ly, T.; Krout, M.; Pham, D. K.; Tani, K.; Stoltz, B. M.; Julian, R. R. *J. Am. Chem. Soc.* **2007**, *129*, 1864–1865. (b) Tani, K.; Stoltz, B. M. *Nature* **2006**, *441*, 731–734.

geometry about the peptide bond, as demonstrated by a high C–N rotational barrier (~20 kcal/mol) and the propensity for protonation at oxygen over nitrogen.[1,4]

Figure 5.1.1. Resonance stabilization of a typical amide.

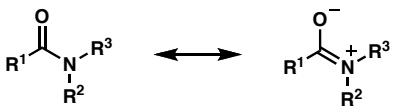

Disruption of the preferred planar geometry dramatically changes the stability and reactivity of the amide functionality. Nonplanar distortions typically lead to increased nitrogen basicity, pyramidalization of nitrogen, increased hydrolytic lability, and selective reactivity of electrophiles with nitrogen.[1,5,6] Though more rare than standard amides, twisted amides are critical design elements in peptide hydrolysis,[7] antibiotic efficacy of β-lactams,[1] and protein folding, with importance in autoimmunosuppression.[8]

5.1.2 2-QUINUCLIDONE

The intriguing qualities of these twisted amides were first recognized in 1938 when one of the simplest families was introduced—molecules containing the 1-azabicyclo[2.2.2]octan-2-one system, the quintessential member being 2-quinuclidone (**311**).[9] In this original report, Lukeš surmised that the most effective way to obtain an amide in twisted conformation is to constrain the nitrogen at the bridgehead of a bicyclic system. Following the report of these "anti-Bredt" lactams,[10] Woodward became interested in the properties of 2-quinuclidone as it related to studies toward quinine (~1941) and later in the context of the structural elucidation of penicillin.[11] The

Woodward laboratory's inability to synthesize **311** from amino acid **310** was attributed to the unstable nature of this amide bond (Figure 5.1.2a), and was supported by the ease of the construction of constitutional isomer **313** from **312** (Figure 5.1.2b).[11a] These observations were of significance to the penicillins, as they indicated that their characteristic reactivity arises not only from ring strain of the β-lactam, but also as a result of nonplanar amide distortions in the fused bicycle.

*Figure 5.1.2. a) Woodward's failed synthesis of **311** from amino acid **310**. b) Facile amide bond formation to afford constitutional isomer **313**.*

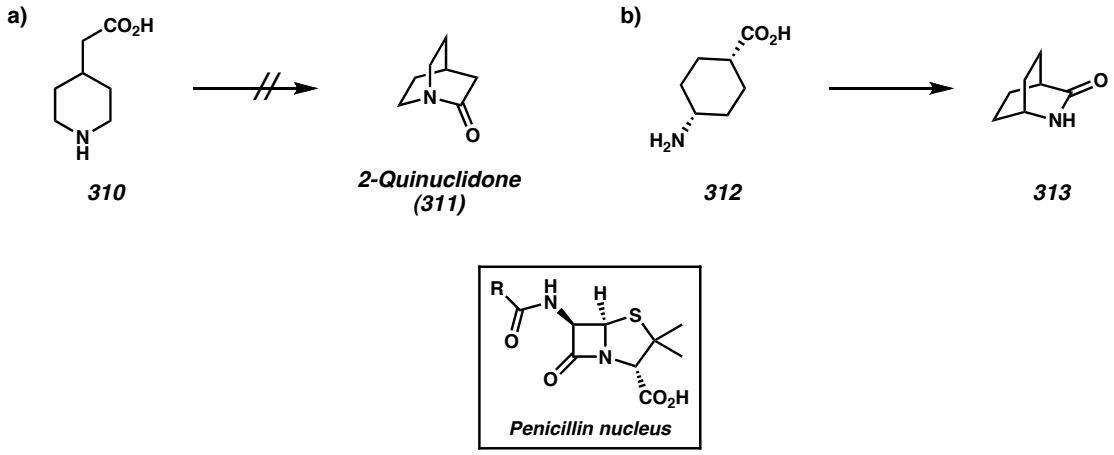

Subsequent studies toward 2-quinuclidone included a report by Yakhontov[12] that claimed to have synthesized **311** using the Woodward approach for amide bond formation. The formation of the strained bicyclic lactam proceeded surprisingly with an aqueous workup, with the reported product (**311**) characterized only by elemental analysis for nitrogen. A later study by Pracejus[13] failed to isolate **311** by the method of Yakhontov, calling the original synthesis into question. However, the preparation of a variety of methyl-substituted 2-quinuclidone derivatives (**315**–**318**) using the amino acid

cyclization approach supported the notion that the original Yakhontov synthesis was flawed, at least in the isolation of **311** (Scheme 5.1.1).[14]

Scheme 5.1.1. Synthesis of methyl-substituted 2-quinuclidone derivatives

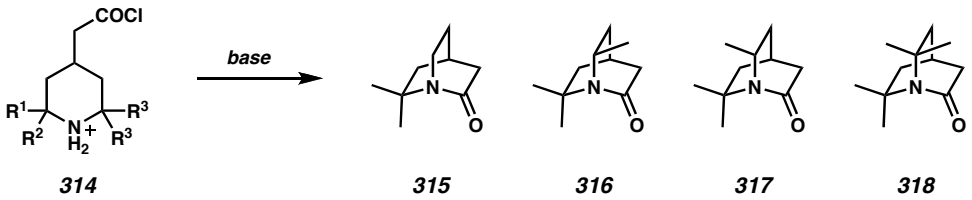

Although the definitive characterization and isolation of **311** has remained elusive despite its apparent simplicity,[6c,15] this quintessential twisted amide has been the subject of computational investigations.[4,16] Studies of this model amide are of particular interest to explore the significance of this distortion phenomenon to provide insights into a number of research areas.[5] Owing to the colorful history[11c,17] and challenges associated with the preparation, isolation, characterization of **311**, we pursued a synthesis using an alternative approach to the classic route for amide bond formation.

5.2 THE SYNTHESIS AND CHARACTERIZATION OF 2-QUINUCLIDONIUM TETRAFLUOROBORATE

In this section we describe our synthetic approach that has enabled the unambiguous preparation and characterization of the quintessential twisted amide 2-quinuclidone (**311**) as its HBF_4 salt. The studies presented in section 5.2 are a partial account of work performed by Dr. Kousuke Tani.[18]

5.2.1 SYNTHESIS OF 2-QUINUCLIDONIUM VIA AN INTRAMOLECULAR SCHMIDT–AUBÉ CYCLIZATION

At the outset of these studies, a strategy was considered that refrained from the use of typical peptide coupling reagents to aid in purification of the likely reactive molecule. It was envisioned that reactions that harnessed the release of dinitrogen could impart significant driving force to assemble the strained bicyclic system. One such approach[19] that met these criteria was the intramolecular Schmidt–Aubé cyclization of ketoazide **320**, which has seen wide use for the synthesis of N-substituted lactams since its initial discovery (Scheme 5.2.1).[20] Moreover, this method recently has been used for the preparation of other types of twisted lactams.[21]

Scheme 5.2.1. Retrosynthetic analysis of 2-quinuclidone using the Schmidt–Aubé reaction

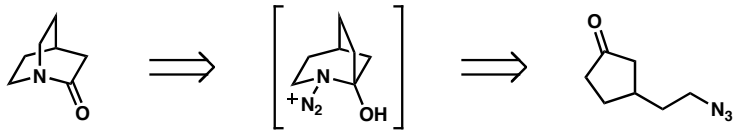

311 ***319*** ***320***

The preparation of ketoazide **320** was accomplished as shown in Scheme 5.2.2. Bayer–Villiger oxidation of norcamphor (**321**) provided bicyclic lactone **322** that was reduced with $LiAlH_4$ to generate *syn*-diol **323** in good yield. Selective tosylation of **323** and S_N2 displacement with sodium azide produced azide **325**. Alcohol oxidation using Dess–Martin periodinane afforded the requisite ketoazide **320**.

Scheme 5.2.2. Preparation of ketoazide ***320***

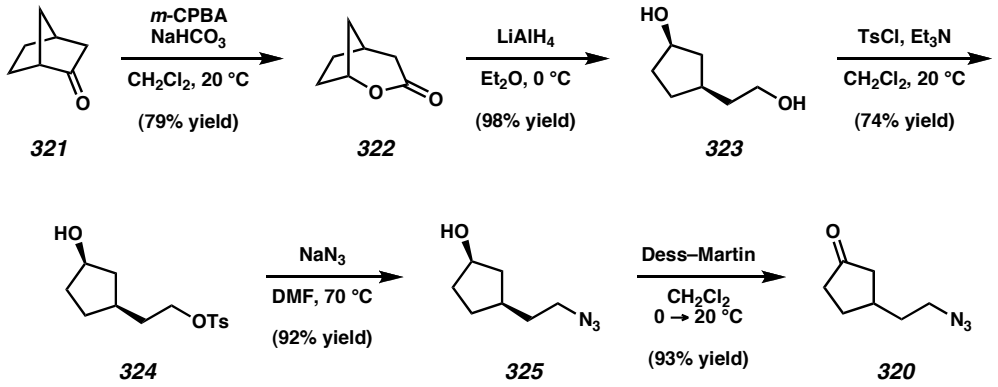

Initial studies toward the intramolecular Schmidt–Aubé reaction of ketoazide **320** demonstrated that a selection of strong acids (e.g., TFA, TfOH, HBF_4, and Tf_2NH) produced a noticeable gas evolution with consumption of **320**. A survey of various acids and solvents established HBF_4 in Et_2O as the optimal conditions for the transformation of **320** into isomeric bicyclic lactams **311**•HBF_4 and **326**•HBF_4 (76:24, respectively).[22] The observation of the two structural isomers **311**:**326** in ~3:1 ratio of indicated a moderately selective C–N migration of bond *a* from intermediate **319** to generate 2-quinuclidonium tetrafluoroborate (**311**•HBF_4) as a major reaction component, whereas minor product **326**•HBF_4 is derived from migration of bond *b* from **319**. The crystallinity of the crude lactams facilitated purification by selective recrystallization with MeCN/Et_2O to afford pure 2-quinuclidonium tetrafluoroborate (**311**•HBF_4) as colorless crystals.

*Scheme 5.2.3. Synthesis of 2-quinuclidonium tetrafluoroborate (**311**•HBF_4)*

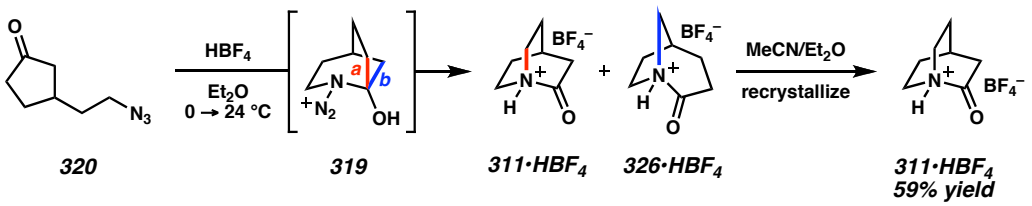

5.2.2 CHARACTERIZATION, PROPERTIES, AND REACTIVITY

The structure of **311**•HBF_4 was unambiguously determined by spectroscopic evaluation. The carbonyl infrared absorption band for **311**•HBF_4 was observed at 1822 cm^{-1} (KBr). This value compares well with the HCl salts of known [2.2.2]bicyclic lactams **316**[13] and **318**[14c] (1818 and 1811 cm^{-1}, respectively) and is more consistent with that of an acid chloride (1820–1750 cm^{-1}) or anhydride (1870–1770 cm^{-1}) than an amide (1690–1650 cm^{-1}).[23] Additionally, the ^{13}C chemical shift of the carbonyl group was observed at δ 175.9 ppm (CD_3CN). Crystals suitable for X-ray analysis enabled the identification of all hydrogens from the electron density map. The structure depicted in Figure 5.2.1 shows that **311**•HBF_4 exists in the N-protonated form, which has been supported by calculations (see subsection 5.3.1) and highlights the twisted nature of the amide.

*Figure 5.2.1. ORTEP drawing of **311**•HBF_4 (shown with 50% probability ellipsoids; BF_4 omitted for clarity).*

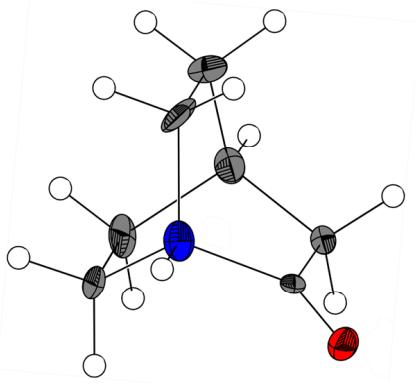

Table 5.2.1 summarizes selected bond lengths and distortion parameters obtained from the X-ray structure of **311**•HBF_4 and previously calculated structures. Two crystallographically independent molecules corresponding to **311**•HBF_4 were observed in the unit cell. The observed bond lengths for the N–C(O) were 1.526 and 1.484 Å while the C=O bond lengths were 1.192 and 1.168 Å. These distances are in good agreement to calculated values for N-protonated **311**•H^+ and show a minimal decrease in the length of C=O bond while the N–C(O) bond is significantly longer than a typical amide (cf. formamide).[4b,15c] Winkler and Dunitz have described distortion parameters for the quantitative evaluation of the twisting of an amide bond, and include the pyramidalization about the nitrogen (χ_N) and carbon (χ_C) atoms and the torsion about the C–N bond (τ).[24] For a representative planar amide (e.g., formamide), these parameters are all 0°.[25] The structures of **311**•HBF_4 possessed a χ_N of 58.9 and 59.5°, while the τ was found to be 90.8 and 90.9°. These values compare well with nonplanar formamide and quantitatively establish the highly twisted nature of **311**•HBF_4.

*Table 5.2.1. Comparison of structural parameters for **311**•HBF_4 and formamide*

	bond lenth (Å)		*distortion parameters (°)*[a]		
compound	N–C(O)	C=O	χ_N	χ_C	τ
311•HBF_4 (X-ray)	1.526(5)	1.192(4)	59.5	0.2	90.9
	1.484(6)	1.168(6)	58.9	–2.4	90.8
311 (N-protonated, calc'd)[b]	1.504	1.167	57.6	0.0	89.9
311 (calc'd)[b]	1.433	1.183	55.6	0.0	90.0
formamide (planar, calc'd)[b,c]	1.349	1.193	0.0	0.0	0.0
formamide (perpendicular, calc'd)[b,c]	1.423	1.179	63.4	0.0	90.0

[a] Ref 24. [b] Ref 4. [c] Ref 25.

The reactivity of 2-quinuclidonium tetrafluoroborate was investigated. **311**•HBF_4 is hypersensitive to hydrolysis, with a $t_{1/2}$ = <15 s in neat D_2O, as well as unstable to manipulations in common nucleophilic solvents (e.g, DMSO, MeOH, pyridine). Furthermore, attempts to neutralize the salt of **311** with various bases lead to the formation of polymeric material, highlighting that the fortuitous protonation of **311** upon Schmidt–Aubé cyclization to **311**•HBF_4 was critical to avoid decomposition. These observations provide further support for the increased reactivity that results from nonplanar distortions of the amide bond.

5.3 GAS-PHASE STUDIES

To gain further insight into twisted amides we explored the gas-phase chemistry of **311**. In this section we present the first experimental results characterizing the basicity of **311**, which is found to be more basic than typical amides. In addition, we report an intriguing gas-phase dissociation as well as a second synthetic route to **311**•H^+, which only occurs in the gas phase.

5.3.1 PROTON AFFINITY VIA THE EXTENDED KINETIC METHOD

The kinetic method, which relies on competitive fragmentation of proton-bound dimers, was employed to determine the proton affinity (PA) of **311** relative to a series of reference bases (shown in Figure 5.3.1) according to previously established methods.[26] Briefly, dimers were introduced into an LTQ linear ion trap mass spectrometer by electrospraying solutions of the tetrafluoroborate salt of **311** in dry acetonitrile and a

reference base. The noncovalently bound dimers were then subjected to collision-induced dissociation (CID) to determine the most basic site (which retains the proton more often). The results are shown in Figure 5.3.1. Analysis of the data yields a PA of 230.6 kcal/mol for **311** using the simple kinetic method. Application of the more rigorous extended kinetic method[27] yields a value of 230.4 kcal/mol, suggesting that entropic effects have a minimal impact on the measured PA. Calculations at the B3LYP 6-311++G** level of theory yield a PA of 225.7 kcal/mol. Previous calculations predicted a PA of 228.9 kcal/mol.[4] Thus **311** is found to be very basic by theory and experiment. By comparison, typical amides have PAs in the range of 210–215 kcal/mol (Figure 5.3.2).[28] In terms of basicity, **311** behaves more like a secondary or tertiary amine owing to the lack of resonance within the amide. In addition, the site of protonation differs for twisted amides with protonation at the nitrogen being favored by ~21.5 kcal/mol according to our calculations.[29] In the process of collecting data to establish the PA of **311**, reference bases were found to separate into two groups. The less bulky bases give the data shown in Figure 5.3.1, which corresponds to dimers that are capable of hydrogen bonding to the nitrogen of **311**. The remaining reference bases are too bulky to access the nitrogen and presumably interact with the carbonyl oxygen of **311**.[30]

*Figure 5.3.1. Data from kinetic method experiments showing the relative PA versus natural log of the ratio of ion intensities minus protonation entropies.[31] Three representative collision energies are shown for each reference base. The collinearity of all three lines indicates few entropic effects. The PA of **311** is determined to be 230.4 kcal/mol by the extended kinetic method.*

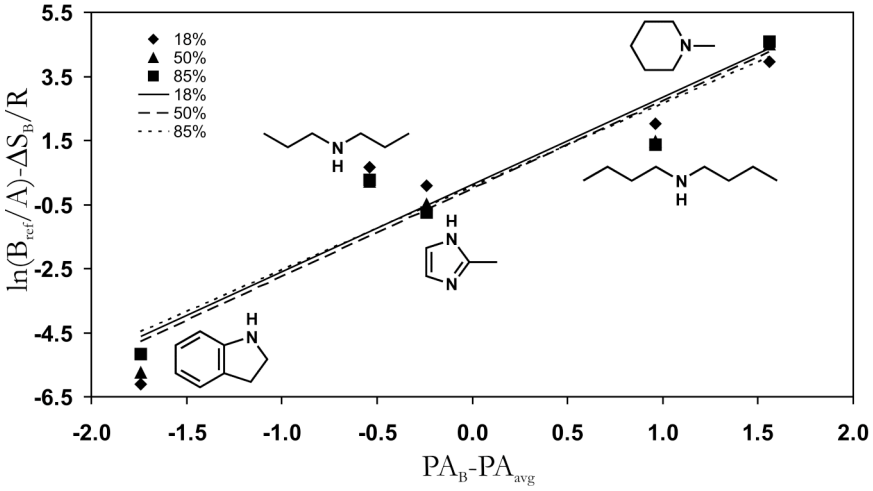

Figure 5.3.2. Representative amide and amine experimentally determined PAs (kcal/mol).

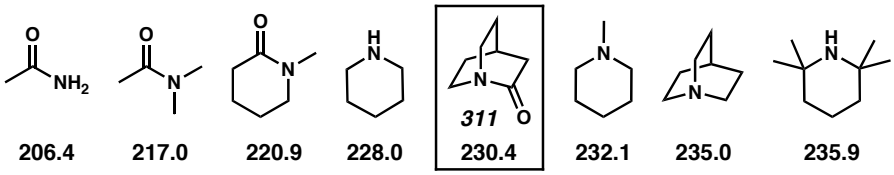

5.3.2 COLLISION-INDUCED DISSOCIATION PATHWAY

The gas-phase properties of 2-quinuclidone (**311**) were explored further by collision-induced dissociation (CID) experiments. The CID spectrum for **311**•H^+ is shown in Figure 5.3.3*i*. Surprisingly, a single loss of 44 Da is the only major product that is observed, indicating that a single fragmentation pathway is energetically favored. Because of the bicyclic nature of **311**•H^+, two covalent bonds must be broken en route to the observed fragmentation. A loss of 44 Da further requires at least one hydrogen

transfer. We propose the mechanism shown in Scheme 5.3.1a to account for the observed loss. Homolytic cleavage of the amide to bond to **327** leads to abstraction of one out of two equivalent hydrogens facing the radical (**327** → **328**). Two possible McLafferty-type[32] rearrangements (one is shown in Scheme 5.3.1a) then lead to the second hydrogen transfer and the production of isomeric dihydropyridiniums **329** and **330** with the loss of ethenol (**331**). In order to verify this mechanism, a series of four compounds labeled with stable isotopes were prepared (**332**–**335**) (Scheme 5.3.1b).

*Figure 5.3.3. i) CID spectrum of **311**•H^+ (m/z = 126) with a single fragment being detected. ii) CID spectrum of **310**•H^+ (m/z = 144). The loss of water generates **311**•H^+, which simultaneously fragments. iii) MS^3 CID spectrum of the reisolated peak at m/z 126 from spectrum ii confirming that **311**•H^+ is generated by the loss of water.*

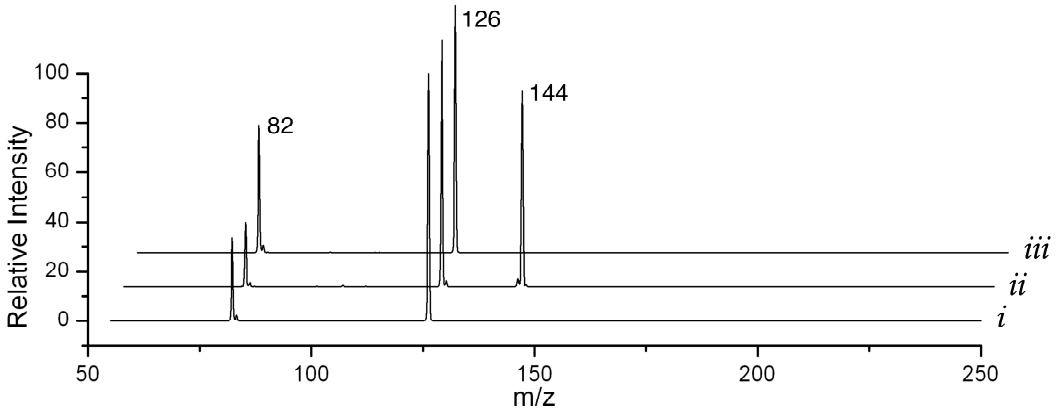

*Scheme 5.3.1. a) Proposed CID fragmentation mechanism of **311**•H⁺. b) Isotopically labeled mechanistic probes*

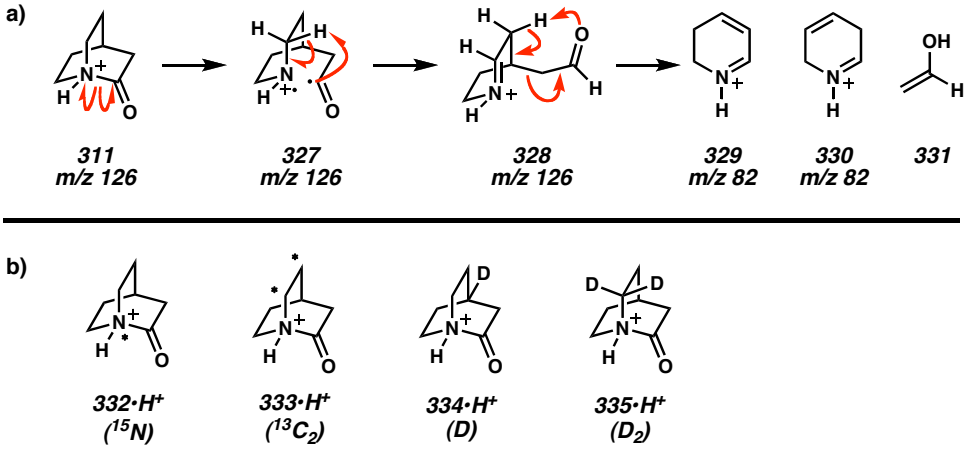

The synthesis of variously labeled derivatives of **311**•HBF_4 is shown in Scheme 5.3.2. Using a route identical to our original synthesis of **311**, substitution of monotosylate **324** with 1-^{15}N-sodium azide and oxidation with Dess–Martin periodinane provided ketoazide **336**, which was subjected to the optimized Schmidt–Aubé conditions, and upon recrystallization, afforded ^{15}N-labeled **332**•HBF_4 (Scheme 5.3.2a). The incorporation of ^{13}C into **311** required a new approach starting from $^{13}C_2$-acetic acid (**337**). Accordingly, Mitsunobu substitution of alcohol **338** generated crystalline ester **339** (Scheme 5.3.2b). Enol silane generation and modified Mukaiyama–Michael addition to cyclopentenone employing buffered TBSOTf constructed ketoester **340** in 79% yield over two steps. Reduction of both carbonyls using $LiAlH_4$, chemoselective oxidation[33] of the secondary alcohol, and mesylation of the resulting primary alcohol yielded ketomesylate **341**. Typical azide substitution and cyclization then gave $^{13}C_2$-labeled **333**•HBF_4. A similar procedure using the conjugate addition with acceptor 3-*d*-cyclopentenone (**342**)[34] provided monodeuterated ketoester **344** that was transformed to D-labeled **334**•HBF_4

over five steps (Scheme 5.3.2c). Reduction of lactone **322** with $LiAlD_4$ and two-step conversion to mesylate **345** enabled the preparation of D_2-labeled **335**•HBF_4 (Scheme 5.3.2d).

*Scheme 5.3.2. Synthetic route for the preparation of isotopically labeled mechanistic probes. a) ^{15}N-labeled **332**•HBF_4; b) $^{13}C_2$-labeled **333**•HBF_4; c) D-labeled **334**•HBF_4; d) D_2-labeled **335**•HBF_4*

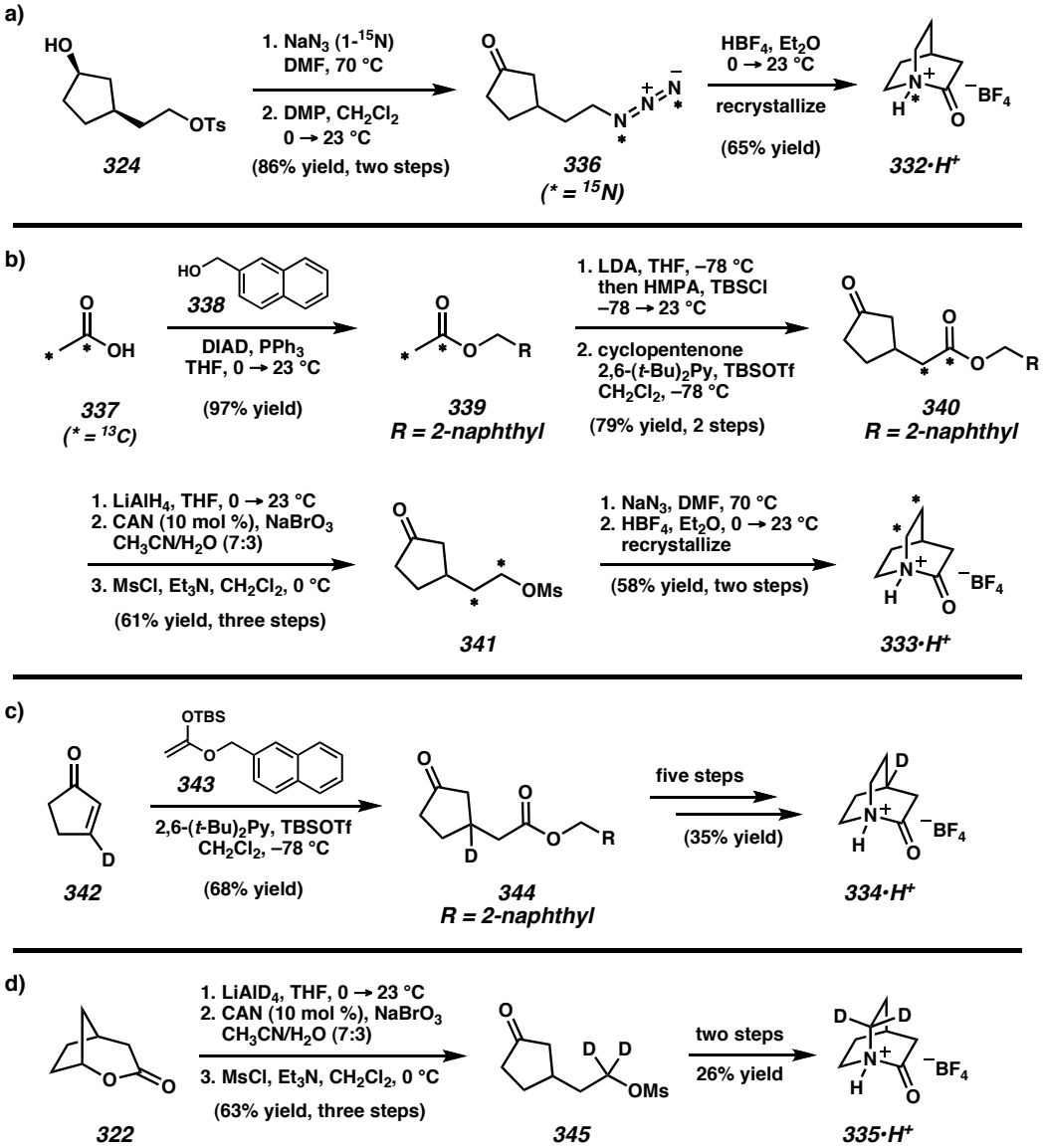

The preparation of various labeled derivatives enabled the verification of our proposed fragmentation mechanism. CID of **332**•H^+ yields a single product that retains the ^{15}N label as expected.[35] Similarly, **333**•H^+ and **334**•H^+ both fragment by yielding a single observable product with both ^{13}C or deuterium labels retained, respectively, in agreement with our mechanism.[35] Additionally, fragmentation of **335**•H^+ confirms that hydrogen transfer occurs.[35] In this case, two products are observed, with the difference between them being the loss of one or retention of two deuteriums. The loss of hydrogen is favored by a factor of 1.7, suggesting that isotope effects[36] may play a role in this reaction. Nevertheless, in each experiment the labeled atoms were lost or retained in agreement with the mechanism shown in Scheme 5.3.1a. As predicted, the amide bond is weakened by the lack of resonance stabilization and is the first bond to break upon collisional excitation.

5.3.3 GAS-PHASE SYNTHESIS OF 2-QUINUCLIDONIUM BY ELIMINATING WATER

Further insight into the chemistry of twisted amides can be obtained by synthesizing them in the absence of solvent. **311**•HBF_4 is observed to rapidly hydrolyze in the presence of water (see subsection 5.2.2), and attempts to drive the reverse reaction in solution have been unsuccessful.[11a] Similarly, attempts to synthesize **311** with the acid chloride of **310** have met with frustration.[13] Nevertheless, collisional excitation of the hydrolyzed derivative **310**•H^+ in the gas phase yields quantitatively a product with the same mass as **311**•H^+ as shown in Figure 5.3.3*ii*. Following reisolation and collisional cooling of this peak, the MS^3 CID spectrum is identical to that obtained by fragmenting

311•H^+ (compare Figure 5.3.3*i* and *iii*). Similarly, all isotopically labeled compounds react exclusively by eliminating water, followed by the same elimination that would be expected if **311**•H^+ were generated as the product.[35] Thus it is possible to selectively synthesize **311**•H^+ by eliminating water from **310**, as shown in Scheme 5.3.3, if the water can be rigorously removed from the reaction system. This is not a difficulty in the gas phase; however, the data in Figure 5.3.3*ii* also suggest that there is a high barrier to this process. Elimination of water to yield **311**•H^+ also results spontaneously in further fragmentation. As mentioned above, this requires the cleavage of two covalent bonds. Therefore, this reaction appears to be difficult in solution for two reasons: a high barrier to activation and back reactions with water.

*Scheme 5.3.3. Gas-phase elimination of water to construct **311**•H^+ and **318**•H^+*

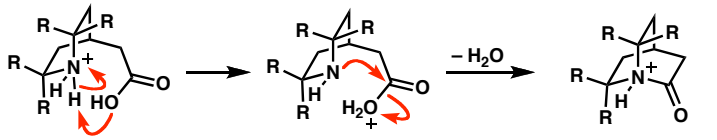

5.3.4 COMPARISON TO 6,6,7,7-TETRAMETHYL-2-QUINUCLIDONE

These results are further confirmed by examination of **318**, which has four additional methyl groups and can be generated from the acid chloride in solution.[13,14d] CID of the hydrolyzed product **346**•H^+ yields exclusively **318**•H^+ without the accompanying loss of additional fragments. The synthesis is again confirmed by comparing fragmentation with the authentic molecule; comparison of Figure 5.3.4*i* with Figure 5.3.4*iii* reveals that even

very low abundance peaks are reproduced. In addition, the voltage amplitude required to carry out the dehydration of **346**•H^+ (Scheme 5.3.3) is 20% lower in magnitude when compared to the voltage required for **310**•H^+. Thus, the energy required to generate **318**•H^+ by eliminating water is much lower, in agreement with the observed synthetic routes in solution. The gas-phase syntheses suggest that **318** is more nucleophilic than **311** and should therefore be more basic as well. Attempts to determine the PA of **318** experimentally by the kinetic method met with frustration. The steric hindrance of the additional methyl groups prevents access to the bridgehead nitrogen. However, theory can be used to estimate the proton affinity. The calculated PA for **318** at the B3LYP/6-311++G** level is 234.7 kcal/mol, which is significantly higher than that for **311** (230.4 kcal/mol) and supports the idea of enhanced nucleophilicity for **318**. The predicted increase in PA with increasing alkyl substitution is evident with the various piperidine derivatives depicted in Figure 5.3.2. However, **318** is also much more stable toward hydrolysis, indicating that stability does not share a simple relationship with basicity for twisted amides.[14d]

Figure 5.3.4. i) CID spectrum of ***318***•H^+ *(m/z = 182). ii) CID spectrum of* ***346***•H^+ *(m/z = 200). In this case, the synthesis proceeds cleanly without spontaneous fragmentation. iii) MS^3 CID spectrum showing that all fragment peaks are reproduced when the gas-phase product is compared to the bona-fide sample in spectrum i.*

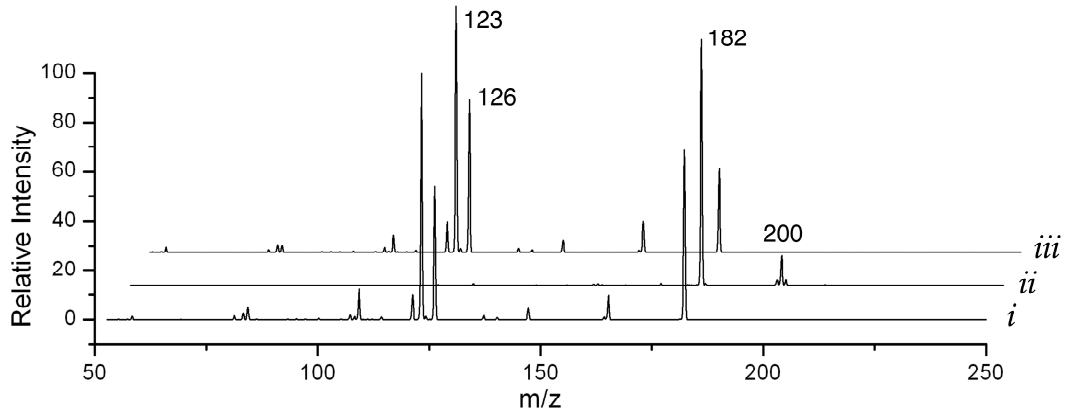

5.4 FUTURE STUDIES

The availability of 2-quinuclidone as its tetrafluoroborate salt (**311**•HBF_4) has enabled the analysis of physical and chemical properties that were previously available only by theoretical calculations.[4] However, experimentation can provide intriguing details and insights beyond what theory can explore as evidenced by subsections 5.3.2–5.3.4. Now that we have a powerful method for the construction of these unique twisted lactams, we can further assess their properties and combine experiment with theory to further the understanding of twisted amides. One particular area of interest is the relationship between the ring size of the bicyclic system and the resulting amide distortion.[4]

5.4.1 1-AZABICYCLO[2.2.1]HEPTAN-2-ONE

We envisioned 1-azabicyclo[2.2.1]heptan-2-one (**349**) in efforts to pursue a more strained derivative of the bridgehead bicyclic lactams (cf. **311**). By analogy, a comparison of ring strains in the parent bicyclic alkane systems reveals that the removal of a carbon from bicyclo[2.2.2]octane (**347**) to bicyclo[2.2.1]heptane (**348**) increases the ring strain from 7.4 to 14.1 kcal/mol, respectively (Figure 5.4.1a).[37] We have calculated the proton affinity of **349** to be 231.7 kcal/mol, which makes it slightly more basic than 2-quinuclidone (**311**) and less basic than tetramethyl derivative **318** (Figure 5.4.1b). This indicates that a predicted increase ring strain affects the nitrogen basicity, although ring strain does not necessarily correlate to an increase in basicity.[4b,38] A detailed theoretical or experimental study of **349** could provide insights into this strained amide.

Figure 5.4.1. a) Comparison of strain energies of related bicyclic systems (kcal/mol).[37] b) Comparison of proton affinity values for select bicyclic twisted amides (kcal/mol).

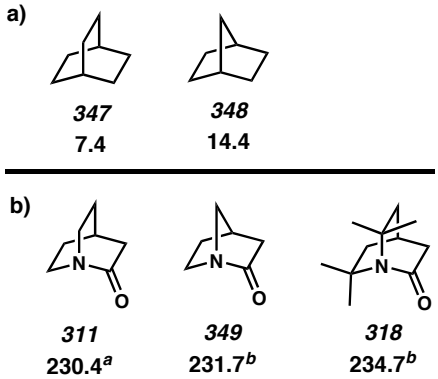

[a] Experimentally determined. [b] Calculated value.

A proposed synthetic route to **349** utilizing the Schmidt–Aubé cyclization is shown in Scheme 5.4.1. Intermolecular [2 + 2] cycloaddition[39] of dichloroketene generated from

350 and Zn(Cu) couple with alkyne **351**[40] should provide dichlorocyclobutenone **352**. Reductive dechlorination and olefin hydrogenation with benzyl cleavage could generate ketoalcohol **353**. Conversion to azide **354** over two steps and subsequent HBF_4-promoted intramolecular cyclization[41] should construct **349•**H^+. The devised synthetic route could enable rapid access to **349** for thorough experimental evaluation.

*Scheme 5.4.1. Proposed synthesis of **349**•H^+ employing the Schmidt–Aubé cyclization*

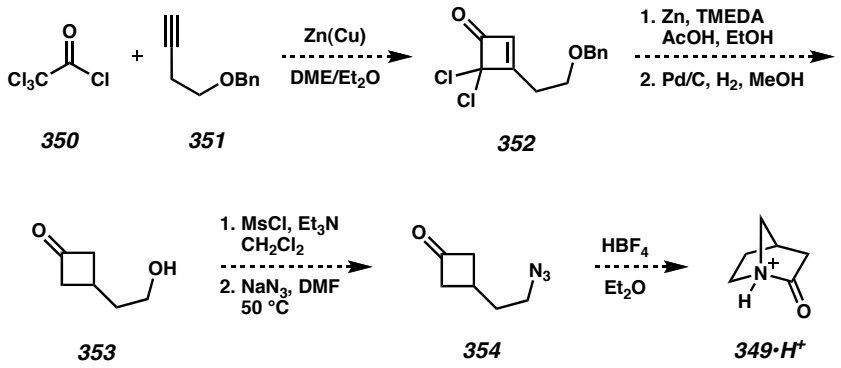

5.4.2 1-AZABICYCLO[3.3.3]UNDECAN-2-ONE

Another interesting example with regard to ring size is the theoretical molecule 1-azabicyclo[3.3.3]undecan-2-one (**355**). The parent amine (manxine, **356**) is extraordinary in that it exhibits a near coplanar geometry about the nitrogen in both neutral and protonated forms.[42] Greenberg has calculated the PA of amide **355** and found that the bicyclo[3.3.3] system favors O-protonation over N-protonation by 3.5 kcal/mol,[4b] suggesting that increase in ring size reduces strain and induces planarity of the nitrogen. As **355** approaches the geometric requirements for an unstrained amide linkage, it has the potential to form a hyperstable amide. The concept of hyperstability, as described by

Schleyer and co-workers for bridgehead olefins,[43] specifies that the strain energy in the enolized lactam is less than that of the parent lactam and could result in interesting reactivity of this larger bicyclic amide.

*Figure 5.4.2. Bicyclo[3.3.3] bridgehead amide **355** and amine **356**.*

355 ***356***

A proposed synthesis of **355** is presented in Scheme 5.4.2. Enolization of vinylogous ester **228** and alkylation with iodide **357**,[44] followed by reductive carbonyl transposition could afford γ-substituted cycloheptenone **358**. Olefin hydrogenation with benzyl cleavage and two-step azide conversion would produce cyclization substrate **359**. Exposure to acidic conditions should facilitate carbonyl addition to intermediate **360** that can undergo a C–N migration in two possible ways to form desired **355** and isomer **361**. The planned route to **355** could provide material to support the evaluation of this intriguing amide.

*Scheme 5.4.2. Proposed synthesis of **355** using the Schmidt–Aubé cyclization*

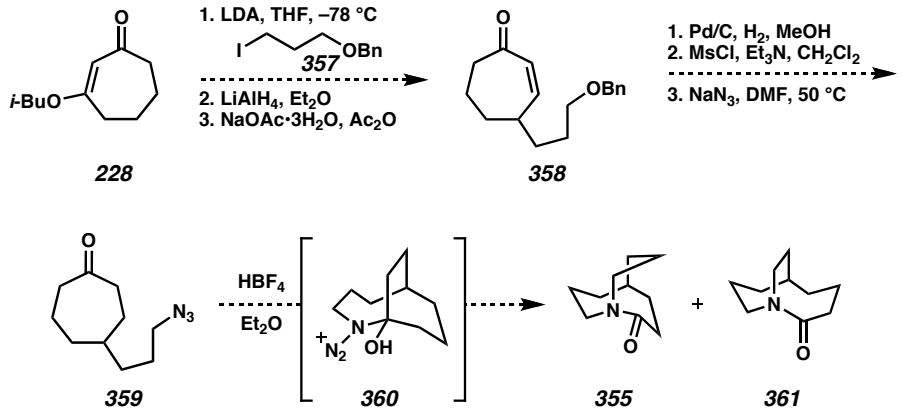

5.5 CONCLUSION

In summary, we have achieved the first unambiguous synthesis, isolation, and X-ray characterization of the quintessential twisted amide 2-quinuclidone (**311**) as its HBF_4 salt. Our synthesis highlights the power of the Schmidt–Aubé reaction for the construction of highly strained amides. We have performed a thorough structural and chemical analysis of **311** and quantitatively established its highly twisted nature. Gas-phase investigations have assessed the basicity of **311** for the first time, revealing an intriguing dissociation mechanism and a second synthesis by eliminating water in the gas phase. Our results indicate that the gas-phase chemistry of these molecules closely reflects the properties observed in solution. Moreover, the studies herein demonstrate the importance of combining theory and experiment to further our understanding of this extraordinary class of compounds. Future studies on the role of ring size and the resulting effect on amide distortion and properties are proposed.

5.6 EXPERIMENTAL SECTION

5.6.1 MATERIALS AND METHODS

5.6.1.1 CHEMICAL SYNTHESIS

Unless stated otherwise, reactions were conducted in flame-dried glassware under an atmosphere of nitrogen using anhydrous solvents passed through activated alumina columns under argon. All commercially obtained reagents were used as received. Hexamethylphosphoramide was distilled from CaH_2 and stored in a Schlenk tube under argon. 3-*d*-cyclopentenone (**342**)[34] and 6,6,7,7-tetramethyl-2-quinuclidone (**318**)[14d] were prepared by known methods. Labeled sodium azide (1-^{15}N, 98 atom% ^{15}N) and acetic acid (**337**, 1,2-$^{13}C_2$, 99 atom% ^{13}C) were purchased from Cambridge Isotope Laboratories. Lithium aluminum deuteride (98 atom% *d*) was purchased from Aldrich. Reaction temperatures were controlled using an IKAmag temperature modulator, and unless stated otherwise, reactions were performed at 23 °C. Thin-layer chromatography (TLC) was conducted with E. Merck silica gel 60 F254 pre-coated plates, (0.25 mm) and visualized using a combination of UV quenching and charring with *p*-anisaldehyde, ceric ammonium molybdate, or potassium permanganate stains. ICN silica gel (particle size 0.032–0.063 mm) was used for flash column chromatography. ^{1}H NMR spectra were recorded on a Varian Mercury 300 (at 300 MHz) or a Varian Inova 500 (at 500 MHz) and are reported relative to Me_4Si (δ 0.0).[45] Data for ^{1}H NMR spectra are reported as follows: chemical shift (δ ppm), multiplicity, coupling constant (Hz) and integration. ^{13}C NMR spectra were recorded on a Varian Mercury 300 (at 75 MHz) or a Varian Inova 500 (at 126 MHz) and are reported relative to Me_4Si (δ 0.0).[45] Data for ^{13}C NMR spectra are

reported in terms of chemical shift, multiplicity, and coupling constant. ^{2}H NMR spectra were recorded on a Varian Inova 500 (at 76 MHz) and are reported relative to Me_4Si (δ 0.0).[45] Data for ^{2}H NMR spectra are reported in terms of chemical shift and multiplicity. IR spectra were recorded on a Perkin Elmer Spectrum BXII spectrometer and are reported in terms of frequency of absorption (cm^{-1}). Melting points are uncorrected. High resolution mass spectra were obtained from the California Institute of Technology Mass Spectral Facility.

5.6.1.2 EXTENDED KINETIC METHOD, GAS-PHASE SYNTHESIS, AND CALCULATIONS

All mass spectra were obtained using an LTQ linear ion trap mass spectrometer (Thermo Electron, Waltham, MA) equipped with a standard electrospray ionization source. Voltages were optimized to maximize the [**311** + H^+ + B_{ref}] dimer peak intensities for kinetic method experiments. All reference bases were purchased from Sigma-Aldrich and were used without further purification.

To minimize hydrolysis of **311**•HBF_4, samples containing 300 μM of **311** and reference base were prepared with dry acetonitrile unless otherwise noted and immediately infused into the electrospray source. The noncovalently bound dimers were then isolated and subjected to CID at normalized collision energies ranging from 18% to 85%. These percentages correspond to excitation voltage amplitudes of 0.00641 to 0.0303 V for a 100 *m/z* ion. To obtain tandem MS data, 30 μM solutions were prepared and analyzed as above under standard instrument tune conditions. Amino acid derivatives were prepared by either allowing a sample sufficient time to hydrolyze (ca.

30 min) or by addition of deionized water in molar excess.

Proton affinities were calculated using hybrid density functional theory as implemented in Gaussian 03 Version 6.1 Revision D.01. Candidate structures were built using GaussView 3.0 and then submitted for optimization and vibrational frequency calculation at the B3LYP/6-31G* level. Total energies were calculated at the B3LYP/6-311++G** level. Total energies, zero point energies (ZPE), and thermal corrections were obtained from the optimization/frequency output. Zero point corrections were scaled by an empirical factor of 0.9877 as recommended by Andersson and Uvdal.[46] The basis set superposition error (BSSE) was calculated using the counterpoise (CP) method of Boys and Bernardi.[47]

5.6.2 PREPARATIVE PROCEDURES

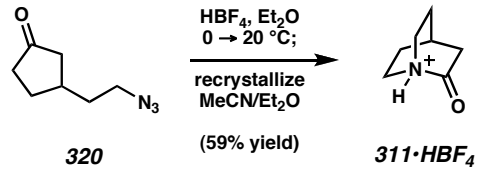

320 *311·HBF4*

2-Quinuclidonium tetrafluoroborate (311•HBF_4). To a solution of **320** (356.5 mg, 2.33 mmol, 1.0 equiv) in Et_2O (4.7 mL, 0.5 M) at 0 °C was added an ethereal solution of HBF_4 (642 μL of a 54 wt % solution, 4.66 mmol, 2.0 equiv) at which time immediate gas evolution was observed. The cooling bath was removed and stirred at room temperature until gas evolution ceased (ca. 8 h) and TLC analysis confirmed consumption of **320**. The supernatant of the resulting suspension was removed by syringe and the remaining white solid was washed with Et_2O (3 x 3 mL) and dried in vacuo. This crude white solid was transferred into a glove box and purified by double recrystallization using slow diffusion of Et_2O into a MeCN solution of the crude. Specifically, the crude was dissolved in a minimal quantity of MeCN, filtered through a pipette with a small filter paper plug, and washed further with minimal MeCN. The resulting vial containing the MeCN solution of the crude was placed in a larger chamber, filled ~1/3 full with Et_2O, and the larger chamber was capped and placed in a –20 °C freezer. After 36–48 h, the chamber was equilibrated to ambient, the supernatant was decanted, and the resulting white solid was washed with excess Et_2O, and recrystallized using the same procedure. Isolation and drying of the resulting solid under vacuum afforded **311**•HBF_4 (292.1 mg, 1.37 mmol, 59% yield) as white needles. Mp = 185–200 ºC dec; ^{1}H NMR (300 MHz, CD_3CN) δ 8.02 (br, 1H), 3.85–3.60 (m, 4H), 2.99 (d, J = 3.0 Hz, 2H), 2.51 (septuplet, J =

3.0 Hz, 1H), 2.10–1.90 (m, 4H); ^{13}C NMR (75 MHz, CD_3CN) δ 175.9, 48.1, 40.1, 25.7, 22.7; IR (KBr) 3168, 2981, 1822, 1468, 1398, 1336, 1312, 948, 823, 799, 766, 716 cm^{-1}; HRMS (FAB+) *m/z* calc'd for $C_7H_{12}NO$ $[M + H]^+$: 126.0919, found 126.0920.

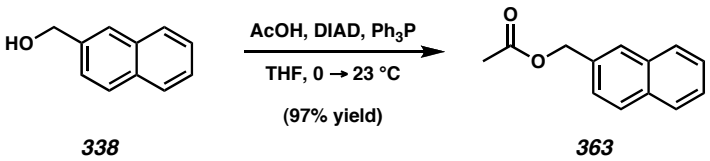

338 ***363***

Naphthalen-2-ylmethyl acetate (363). Ph_3P (0.787 g, 3.0 mmol, 1.5 equiv) and alcohol **362** (0.475 g, 3.0 mmol, 1.5 equiv) were dissolved in THF (13.4 mL, 0.15 M). Acetic acid (114 μL, 2.0 mmol, 1.0 equiv) was added and the solution was cooled to 0 °C in an ice/water bath. DIAD (591 μL, 3.0 mmol, 1.5 equiv) dissolved in THF (1 mL) was added dropwise over 5 min via positive pressure cannulation. After 1 h, the reaction was quenched with 5 mL saturated $NaHCO_3$, extracted with hexanes (3 x 20 mL), the organics were dried over $MgSO_4$, filtered, and concentrated under reduced pressure to an off-white solid. The resulting crude material was purified by flash chromatography on SiO_2 (15:1 → 9:1 hexanes/Et_2O, PhMe loaded) to afford **363** (0.3830 g, 1.91 mmol, 96% yield) as a white solid. R_f = 0.28 (9:1 hexanes/Et_2O); mp = 53–55 °C; ^{1}H NMR (300 MHz, $CDCl_3$) δ 7.89–7.85 (comp m, 4H), 7.53–7.47 (comp m, 3H), 5.30 (s, 2H), 2.16 (s, 3H); ^{13}C NMR (125 MHz, $CDCl_3$) δ 171.1, 133.5, 133.4, 133.3, 128.5, 128.1 (2C), 127.9, 127.5 (2C), 126.5, 126.4, 126.1, 66.6, 21.2; IR (Neat Film NaCl) 3055, 2953, 1736, 1378, 1364, 1248, 1030, 951, 896, 863, 822, 744, 480 cm^{-1}; HRMS (EI+) *m/z* calc'd for $C_{13}H_{12}O_2$ $[M]^+$: 200.0837, found 200.0844.

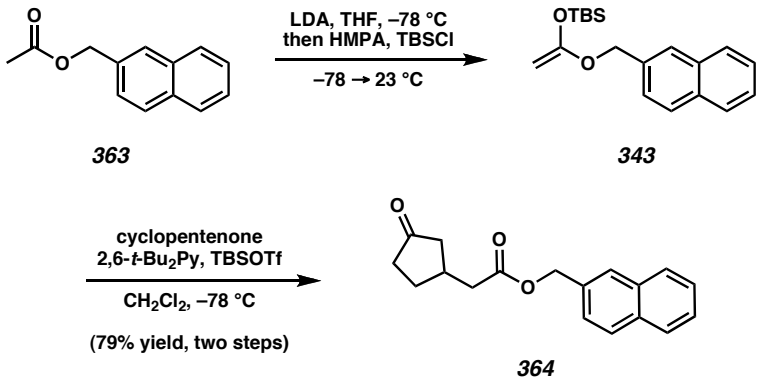

Ketoester 364. To a cooled solution of *i*-Pr_2NH (341 μL, 2.44 mmol, 1.15 equiv) in THF (2.12 mL, 1 M) at 0 °C was added *n*-BuLi (2.5 M in hexane) dropwise. After stirring for 15 min at 0 °C, the solution was cooled to –78 °C and a solution of acetate **363** (424.0 mg, 2.12 mmol, 1.0 equiv) in THF (1 mL) was added dropwise via positive pressure cannulation. After 15 min, HMPA (332 μL, 1.91 mmol, 0.9 equiv), then TBSCl (351.0 mg, 2.33 mmol, 1.1 equiv) in THF (0.80 mL) were added and the cooling bath was removed. The reaction was warmed to ambient temperature and concentrated under reduced pressure. The resulting thick oil was dissolved in 9:1 hexanes/Et_2O (50 mL) and washed with distilled water (3 x 20 mL, pH ≈ 7) and sat. brine. The organic layer was dried over $MgSO_4$, filtered, and concentrated under reduced pressure. The resulting yellow oil solidified after several hours under high vacuum to afford TBS-silylenol ether **343** (650.9 mg), which was used without further purification in the subsequent reaction. *R_f = unstable to SiO_2.*

To a solution of **343** (1.2 equiv), cyclopentenone (145 μL, 1.72 mmol, 1.0 equiv), and 2,6-di-*tert*-butylpyridine (465 μL, 2.07 mmol, 1.2 equiv) in CH_2Cl_2 (20.7 mL, 0.1 M) cooled to –78 °C was added a solution of TBSOTf (475 μL, 2.07 mmol, 1.2 equiv) in CH_2Cl_2 (2.1 mL) dropwise over 15 min. Following consumption of cyclopentenone by TLC analysis (ca. 15 min), the cooling bath was removed and the reaction was quenched

with 15 mL of 3% aq HCl. After stirring for 30 min the layers were separated and the aq layer was extracted with CH_2Cl_2 (3 x 25 mL), the organics dried over $MgSO_4$, filtered, and concentrated under reduced pressure to a yellow solid. The crude product was purified by flash chromatography on SiO_2 (9:1 → 4:1 → 3:1 hexanes/EtOAc, dry load) to afford ketoester **364** (385.4 mg, 1.37 mmol) as a light yellow oil. R_f = 0.23 (1:1 hexanes/Et_2O); ^{1}H NMR (300 MHz, $CDCl_3$) δ 7.87–7.82 (comp m, 4H), 7.53–7.49 (comp m, 2H), 7.45 (dd, *J* = 8.5, 1.9 Hz, 1H), 5.30 (s, 2H), 2.70–2.57 (m, 1H), 2.55 (d, *J* = 1.1 Hz, 1H), 2.53 (d, *J* = 2.9 Hz, 1H), 2.51–2.45 (m, 1H), 2.38–2.11 (comp m, 3H), 1.90 (ddd, *J* = 18.1, 9.8, 1.1 Hz, 1H), 1.66–1.51 (m, 1H); ^{13}C NMR (75 MHz, $CDCl_3$) δ 218.4, 172.0, 133.3 (2C), 133.2, 128.6, 128.1, 127.9, 127.7, 126.5 (2C), 126.0, 66.7, 44.7, 39.9, 38.4, 33.6, 29.4; IR (Neat Film NaCl) 3049, 2956, 1737, 1271, 116, 817 cm^{-1}; HRMS (EI+) *m/z* calc'd for $C_{18}H_{18}O_3$ $[M]^+$: 282.1256, found 282.1257.

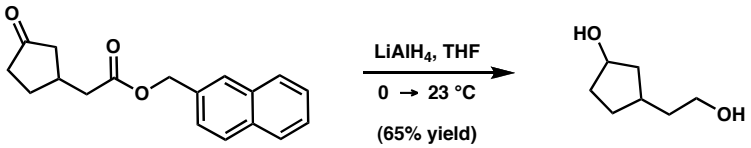

364 ***365***

Diol 365. To a slurry of $LiAlH_4$ (74.3 mg, 1.96 mmol, 4.0 equiv) in THF (4.9 mL, 0.1M) at 0 °C was added ketoester **364** (138.1 mg, 0.498 mmol, 1.0 equiv) in 1.0 mL THF. The cooling bath was removed and the reaction was stirred for 2.5 h at ambient temperature. The reaction was then cooled to 0 °C and carefully quenched by slow addition of Na_2SO_4•$10H_2O$. When gas evolution had ceased, the flask was diluted up to 25 mL with EtOAc and stirred vigorously at ambient temperature for 2 h. The fine precipitate was then filtered through Celite, washing with excess EtOAc, and the

resulting filtrate was concentrated under reduced pressure to an off-white solid. This residue was purified by flash chromatography on SiO_2 (2:1 → 1:0 EtOAc/hexanes) to afford ~1:1 mixture of diastereomers of diol **365** (42.6 mg, 0.320 mmol, 65% yield) as a colorless oil. R_f = 0.15 (3:1 EtOAc/hexanes); ^{1}H NMR (500 MHz, CD_3OD) δ 4.26 (anti diastereomer, app dq, J = 8.4, 2.9 Hz, 0.47H), 4.21 (syn diastereomer, app pentet, J = 5.9 Hz, 0.53H), 3.56 (app t, J = 6.8 Hz, 2H), 2.20 (ddd, J = 16.4, 7.8, 7.8 Hz, 0.53H), 2.14 (ddd, J =14.2, 7.6, 7.6 Hz, 0.53H), 1.98–1.90 (comp m, 1.5H), 1.81–1.72 (comp m, 1.5H), 1.65–1.60 (comp m, 1.5H), 1.59–1.51 (comp m, 1.5H), 1.44–1.31 (m, 1H), 1.19–1.12 (m, 1H); ^{13}C NMR (125 MHz, CD_3OD) δ 74.1 (syn), 62.2, 62.1 (syn), 43.1, 42.9 (syn), 40.6 (syn), 40.1, 36.1 (syn), 35.8 (syn), 35.6, 35.2, 31.5, 31.2 (syn); IR (Neat Film NaCl) 3323 (br), 2931, 2864, 1434, 1344, 1052, 1013 cm^{-1}; HRMS (EI+) *m/z* calc'd for $C_7H_{14}O_2$ $[M]^+$: 130.0994, found 130.0994.

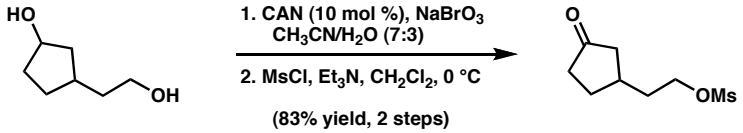

365 ***366***

Ketomesylate 366.[33] To a solution of diol **365** (87.6 mg, 0.673 mmol, 1.0 equiv) in CH_3CN (2.8 mL, 0.167 M) in a vial was added CAN (36.9 mg, 0.673 mmol, 0.1 equiv), $NaBrO_3$ (101.5 mg, 0.673 mmol, 1.0 equiv), and distilled H_2O (1.2 mL) and vigorously stirred. Following consumption of diol **365** by TLC (ca. 6 h), the reaction was concentrated under reduced pressure. The resulting slurry was taken up in 10 mL H_2O, extracted with EtOAc (3 x 25 mL), dried over Na_2SO_4, filtered, and concentrated under reduced pressure to afford a crude yellow oil (85.5 mg).

The resulting crude material was dissolved in CH_2Cl_2 (1.35 mL, 0.5 M), cooled to 0 °C, and MsCl (77.4 μL, 1.0 mmol, 1.5 equiv) and Et_3N (167 μL, 1.2 mmol, 1.8 equiv) were added sequentially. After 5 min, the reaction was quenched with saturated aq $NaHCO_3$ (1 mL) and diluted up to 10 mL with CH_2Cl_2. The biphasic solution was further diluted with sat. aq $NaHCO_3$ (2 mL) and sat. brine (2 mL), the layers were separated, and the aq layer was extracted with CH_2Cl_2 (3 x 10 mL). The combined organics were dried over $MgSO_4$, filtered, and concentrated to a light yellow solid under reduced pressure. This residue was purified by flash chromatography on SiO_2 (2:1 → 1:2 hexanes/EtOAc, dry load) to afford ketomesylate **366** (115.4 mg, 0.560 mmol, 83% yield over two steps) as a colorless oil. R_f = 0.31 (3:1 EtOAc/hexanes); ^{1}H NMR (300 MHz, $CDCl_3$) δ 4.29 (app dt, *J* = 6.4, 2.4, 2.4 Hz, 2H), 3.02 (s, 3H), 2.51–2.42 (m, 1H), 2.40–2.12 (comp m, 4H), 1.95–1.89 (comp m, 2H), 1.84 (ddd, *J* = 17.6, 7.7, 1.3 Hz, 1H), 1.64–1.48 (m, 1H); ^{13}C NMR (75 MHz, $CDCl_3$) δ 218.3, 68.2, 44.8, 38.5, 37.6, 35.0, 33.8, 29.4; IR (Neat Film NaCl) 3023, 2935, 1737, 1350, 1173, 954 cm^{-1}; HRMS (EI+) *m/z* calc'd for $C_8H_{14}O_4S$ $[M]^+$: 206.0613; found 206.0622.

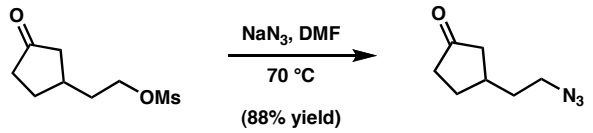

366 ***320***

Ketoazide 320. To a solution of mesylate **366** (50.2 mg, 0.243 mmol, 1.0 equiv) in DMF (0.50 mL, 0.5 M) was added NaN_3 (17.4 mg, 0.268 mmol, 1.1 equiv), and the mixture was warmed to 70 °C until consumption of **366** by TLC. The reaction was cooled to 0 °C and stirred for 15 min, followed by dilution with Et_2O. The suspension was filtered through a plug of Celite with Et_2O, concentrated under reduced pressure, and purified by

flash chromatography SiO_2 (6:1 → 3:1 hexanes/Et_2O, PhMe load) to afford ketoazide **320** (32.8 mg, 0.214 mmol, 88% yield) as a colorless oil. R_f = 0.25 (3:1 hexanes/EtOAc); ^1H NMR (300 MHz, $CDCl_3$) δ 3.36 (t, J = 7.1 Hz, 2H), 2.50–2.10 (m, 5H), 1.90–1.70 (m, 3H), 1.54 (m, 1H). All other spectral data are consistent with reported values.

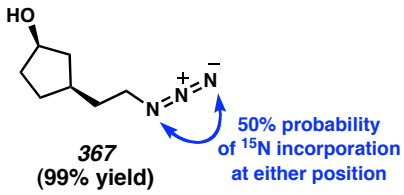

(^{15}N)-labeled azidoalcohol 367. Prepared by a known method using (1-^{15}N)-NaN_3. The reaction was purified by flash chromatography on SiO_2 (3:1 → 1:1 hexanes/Et_2O, PhMe load) to afford ^{15}N-labeled azidoalcohol **367** (186.1 mg, 1.19 mmol, 99% yield) as colorless oil. R_f = 0.14 (1:1 hexanes/Et_2O); IR (Neat Film NaCl) 3344, 2946, 2868, 2074, 1339, 1243 cm^{-1}; HRMS (FAB+) m/z calc'd for $C_7H_{14}N_2O^{15}N$ $[M + H]^+$: 157.1107, found 157.1141. All other spectral data are consistent with reported values.

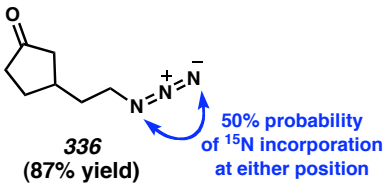

(^{15}N)-labeled ketoazide 336. Prepared by a known method. The reaction was purified by flash chromatography on SiO_2 (6:1 → 3:1 hexanes/Et_2O) to afford ketoazide **336** (155.5 mg, 1.00 mmol, 87% yield) as colorless oil. R_f = 0.26 (1:1 hexanes/Et_2O); IR (Neat Film NaCl) 2931, 2873, 2076, 1740, 1242, 1160 cm^{-1}. All other spectral data are consistent with reported values.

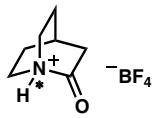

50% ^{15}N incorporation

332•HBF$_4$
(65% yield)

1-^{15}N-2-quinuclidonium tetrafluoroborate (332•HBF$_4$). Prepared by a known method. The crude reaction precipitate was transferred to a glove box and recrystallized twice by slow diffusion of Et_2O into CH_3CN at –20 °C to afford **332•**HBF_4 (127.7 mg, 0.598 mmol, 65% yield) as white needles. HRMS (FAB+) *m/z* calc'd for $C_7H_{12}O^{15}N$ $[M + H]^+$: 127.0889, observed 127.0855; *m/z* calc'd for $C_7H_{12}NO$ $[M + H]^+$: 126.0919, observed 126.0915; relative peak ratio = 1:1.

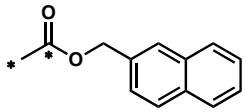

339
(97% yield)

$^{13}C_2$-labeled acetate 339. Prepared as above to afford **339** (0.8326 g, 4.12 mmol, 97% yield) as an off-white solid. Mp = 54–56 °C; ^{1}H NMR (300 MHz, $CDCl_3$) δ 7.87–7.83 (comp m, 4H), 7.53–7.45 (comp m, 3H), 5.27 (d, J_{H-13C} = 3.2 Hz, 2H), 2.13 (dd, J_{H-13C} = 129.7, 6.9 Hz); ^{13}C NMR (75 MHz, $CDCl_3$) δ 170.9 (d, $J_{13C-13C}$ = 59.4 Hz), 21.1 (d, $J_{13C-13C}$ = 59.2 Hz); IR (Neat Film NaCl) 3054, 2955, 1693, 1360, 1276, 1218, 1024, 970, 951, 897, 864, 823, 744 cm^{-1}; HRMS (EI+) *m/z* calc'd for $C_{11}H_{12}O_2{}^{13}C_2$ $[M]^+$: 202.0904, found 202.0913.

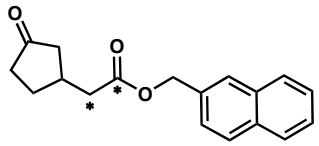

340
(79% yield)

$^{13}C_2$-labeled ketoester 340. Prepared as above to afford **340** (0.4204 g, 1.42 mmol, 79% yield) as a pale yellow oil. ^{1}H NMR (300 MHz, $CDCl_3$) δ 7.87–7.82 (comp m, 4H), 7.53–7.49 (comp m, 2H), 7.45 (dd, *J* = 8.5, 1.6 Hz, 1H), 5.30 (d, *J* = 3.2 Hz, 2H), 2.54 (dddd, J_{H-13C} = 129.2, 6.9 Hz, *J* = 10.9, 2.0 Hz, 2H), 2.71–2.58 (m, 1H), 2.49 (ddd, *J* = 16.8, 7.4 Hz, J_{H-13C} = 1.3 Hz, 1H), 2.28–2.11 (comp m, 3H), 1.96 (dddd, *J* = 18.1, 10.4, 5.3 Hz, J_{H-13C} = 1.3 Hz, 1H), 1.67–1.50 (m, 1H); ^{13}C NMR (75 MHz, $CDCl_3$) δ 172.0 (d, $J_{13C-13C}$ = 57.2 Hz), 39.9 (d, $J_{13C-13C}$ = 57.5 Hz); IR (Neat Film NaCl) 3054, 2958, 1740, 1690, 1403, 1150, 1124, 818, 754 cm^{-1}; HRMS (EI+) *m/z* calc'd for $C_{16}H_{18}O_3{}^{13}C_2$ $[M]^+$: 284.1323, found 284.1322. All other spectral data are consistent with reported values.

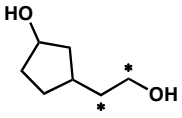

368
(74% yield)

$^{13}C_2$-labeled diol 368. Prepared as above to afford ~1:1 mixture of diastereomers of **368** (54.9 mg, 0.415 mmol, 74% yield) as a colorless oil. ^{1}H NMR (300 MHz, CD_3OD) δ 4.26 (dddd, *J* = 5.6, 5.6, 2.9, 2.9 Hz, 0.44H), 4.21 (dddd, *J* = 4.8, 4.8, 4.8, 4.8, 0.56 H), 3.56 (dddd, J_{H-13C} = 140.2, 6.9 Hz, *J* = 6.9, 2.4 Hz, 2H), 2.18–2.09 (m, 1H), 2.0–1.7 (comp m, 3H), 1.65–1.49 (m, 1H), 1.46–1.28 (comp m, 2H), 1.23–1.09 (m, 1H); ^{13}C NMR (75 MHz, CD_3OD) δ 62.2 (d, $J_{13C-13C}$ = 37.3 Hz, 0.44C), 62.1 (d, $J_{13C-13C}$ = 37.3 Hz,

0.56C), 40.6 (d, $J_{13C–13C}$ = 37.3 Hz, 0.56C), 40.1 (d, $J_{13C–13C}$ = 37.3 Hz, 0.44C). All other spectral data are consistent with reported values.

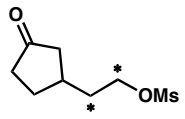

341
(83% yield, two steps)

$^{13}C_2$-labeled ketomesylate 341. Prepared as above to afford **341** (71.7 mg, 0.344 mmol, 83% yield over two steps) as a colorless oil. ^{1}H NMR (300 MHz, $CDCl_3$) δ 4.30 (dddd, $J_{H–13C}$ = 149.4, 6.4 Hz, J = 6.4, 2.7 Hz, 2H), 3.03 (s, 3H), 2.47 (ddd, J = 17.8, 7.5 Hz, $J_{H–13C}$ = 1.0 Hz, 1H), 2.41–2.08 (comp m, 5H), 1.85 (dddd, J = 17.8, 10.1, 5.1 Hz, $J_{H–13C}$ = 1 Hz, 1H), 1.74–1.66 (m, 1H), 1.63–1.52 (m, 1H); ^{13}C NMR (75 MHz, $CDCl_3$) δ 68.1 (d, $J_{13C–13C}$ = 37.9 Hz), 35.0 (d, $J_{13C–13C}$ = 38.2 Hz); HRMS (EI+) *m/z* calc'd for $C_6H_{14}SO_4{}^{13}C_2$ $[M]^+$: 208.0680, found 208.0688. All other spectral data are consistent with reported values.

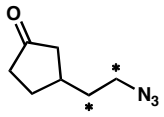

369
(96% yield)

$^{13}C_2$-labeled ketoazide 369. Prepared as above to afford **369** (28.5 mg, 0.184 mmol, 96% yield) as a colorless oil. ^{1}H NMR (300 MHz, $CDCl_3$) δ 3.36 (app ddt, $J_{H–13C}$ = 141.4, 6.9 Hz, J = 3.2 Hz, 2H), 2.44 (dd, J = 17.8, 8.0 Hz, 1H), 2.37–2.11 (comp m, 4H), 2.00–1.91 (m, 1H), 1.83 (ddd, J = 17.6, 9.8, 4.8 Hz, 1H), 1.62–1.49 (comp m, 2H); ^{13}C NMR

(75 MHz, $CDCl_3$) δ 50.0 (d, $J_{13C–13C}$ = 36.8 Hz), 34.6 (d, $J_{13C–13C}$ = 36.8 Hz). All other spectral data are consistent with reported values.

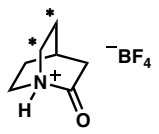

333
(60% yield)

5,6-$^{13}C_2$-2-quinuclidonium tetrafluoroborate (333•HBF_4). Prepared as above to afford **333**•HBF_4 (36.5 mg, 0.170 mmol, 60% yield) as white needles. ^{1}H NMR (300 MHz, CD_3CN) δ 7.99 (br s, 1H), 3.69 (m, 2H), 3.69 (m, $J_{H–13C}$ = 150.4 Hz, 2H), 2.97 (app d, J = 5.4, 3.3 Hz, 3H), 2.55–2.47 (m, 1H), 1.98 (m, 2H), 1.98 (m, $J_{H–13C}$ = 135.4 Hz, 2H); ^{13}C NMR (75 MHz, CD_3CN) δ 47.9 (d, $J_{13C–13C}$ = 32.6 Hz), 22.6 (d, $J_{13C–13C}$ = 32.6 Hz); HRMS (FAB+) *m/z* calc'd for $C_5H_{12}NO^{13}C_2$ $[M + H]^+$: 128.0986, observed 128.0960.

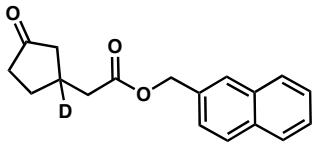

344
(68% yield)

D-labeled ketoester 344. Prepared as above to afford **344** (0.3283 g, 1.15 mmol, 68% yield) as a pale yellow oil. ^{1}H NMR (300 MHz, $CDCl_3$) δ 7.87–7.82 (comp m, 4H), 7.53–7.49 (comp m, 2H), 7.45 (dd, J = 8.5, 1.6 Hz, 1H), 5.30 (s, 2H), 2.53 (dd, J = 16.6, 16.6 Hz, 2H), 2.48 (d, J = 18.6 Hz, 1H), 2.37–2.11 (comp m, 3H), 1.89 (d, J = 18.6 Hz, 1H), 1.64–1.51 (m, 1H); ^{13}C NMR (75 MHz, $CDCl_3$) δ 218.4, 172.0, 133.3 (2C), 128.6, 128.1, 127.9, 127.6, 126.5 (2C), 126.0, 66.7, 44.6, 39.7, 38.4, 33.2 (t, J_{CD} = 20.2 Hz),

29.2; ^{2}H NMR (76 MHz, $CHCl_3$) δ 2.66 (s); HRMS (EI+) *m/z* calc'd for $C_{18}H_{17}O_3{}^{2}H$ $[M]^+$: 283.1319, found 283.1323. All other spectral data are consistent with reported values.

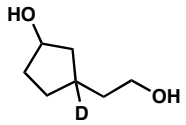

370
(71% yield)

D-labeled diol 370. Prepared as above to afford ~1:1 mixture of diastereomers of **370** (46.0 mg, 0.351 mmol, 71% yield) as a colorless oil. ^{1}H NMR (300 MHz, CD_3OD) δ 4.26 (ddd, *J* = 8.2, 3.5, 2.4 Hz, 0.45H), 4.21 (ddd, *J* = 11.3, 6.4, 6.4 Hz, 0.55H), 3.56 (app t, *J* = 6.9 Hz, 2H), 2.13 (dd, *J* = 13.3, 6.4 Hz, 0.45H), 1.99–1.88 (m, 0.55H), 1.82–1.70 (comp m, 2H), 1.59 (dt, *J* = 22.3, 6.9, 3H), 1.44–1.30 (m, 1H), 1.14 (dd, *J* = 12.0, 4.5 Hz, 1H): ^{13}C NMR (75 MHz, CD_3OD) δ 74.1, 62.2, 62.1, 43.0, 42.7, 40.5, 40.0, 35.8, 35.6, 35.6 (t, J_{CD} = 19.5 Hz), 34.8 (t, J_{CD} = 19.5 Hz), 31.4, 31.1; ^{2}H NMR (76 MHz, CH_3OH) δ 2.14 (s), 1.87 (s). All other spectral data are consistent with reported values.

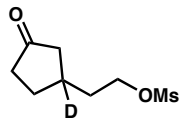

371
(83% yield, two steps)

D-labeled ketomesylate 371. Prepared as above to afford **371** (60.3 mg, 0.291 mmol, 83% yield over two steps) as a colorless oil. ^{1}H NMR (300 MHz, $CDCl_3$) δ 4.30 (app dt, *J* = 6.1, 2.7 Hz, 2H), 3.03 (s, 3H), 2.46 (d, *J* = 18.1 Hz, 1H), 2.40–2.12 (comp m, 3H), 1.91 (app t, *J* = 6.4 Hz, 2H), 1.85 (d, *J* = 18.6 Hz, 1H), 1.61–1.50 (m, 1H); ^{13}C NMR (75 MHz, $CDCl_3$) δ 218.3, 68.1, 44.7, 38.5, 37.7, 34.9, 33.4 (t, J_{CD} = 19.8 Hz),

29.3; ^{2}H NMR (76 MHz, $CHCl_3$) δ 2.35 (s); HRMS (EI+) *m/z* calc'd for $C_8H_{13}O_4S^2H$ $[M]^+$: 207.0676, found 207.0673. All other spectral data are consistent with reported values.

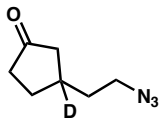

372
(88% yield)

D-labeled ketoazide 372. Prepared as above to afford **372** (39.3 mg, 0.255 mmol, 88% yield) as a colorless oil. ^{1}H NMR (300 MHz, $CDCl_3$) δ 3.36 (ddd, *J* = 6.8, 6.8, 2.9 Hz, 2H), 2.43 (d, *J* = 18.3 Hz, 1H), 2.36–2.30 (m, 1H), 2.23–2.14 (comp m, 2H), 1.83 (d, *J* = 18.1 Hz, 1H), 1.74 (ddd, *J* = 6.8, 6.8, 3.7 Hz, 2H), 1.58–1.51 (m, 1H); ^{13}C NMR (125 MHz, $CDCl_3$) δ 218.6, 50.0, 44.8, 38.5, 34.6, 34.3 (t, J_{CD} = 19.8 Hz), 29.4; ^{2}H NMR (76 MHz, $CHCl_3$) δ 2.29 (s). All other spectral data are consistent with reported values.

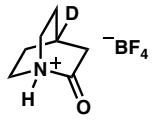

334•HBF4
(67% yield)

4-*d*-2-quinuclidonium tetrafluoroborate (334•HBF_4). Prepared as above to afford **334**•HBF_4 (33.0 mg, 0.154 mmol, 67% yield) as white needles. ^{1}H NMR (300 MHz, CD_3CN) δ 7.95 (br s, 1H), 3.78–3.58 (m, 4H), 2.96 (s, 2H), 2.00–1.95 (m, 4H); ^{2}H NMR (76 MHz, CH_3CN) δ 2.49 (s); HRMS (FAB+) *m/z* calc'd for $C_7H_{11}NO^2H$ $[M + H]^+$: 127.0982, observed 127.0943.

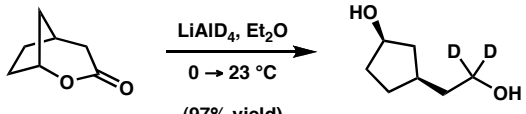

322 ***373***

D_2-labeled *syn*-diol 373. Prepared by a known method using $LiAlD_4$. *syn*-Diol **373** isolated as a colorless oil (0.6317 g, 4.78 mmol, 97% yield) with >98% *d*-incorporation. ^{1}H NMR (300 MHz, CD_3OD) δ 4.21 (dddd, *J* = 5.8, 5.8, 5.8, 5.8 Hz, 1H), 2.14 (ddd, *J* = 13.6, 7.2, 7.2 Hz, 1H), 2.01–1.85 (m, 1H), 1.83–1.70 (comp m, 2H), 1.64–1.55 (comp m, 3H), 1.48–1.31 (m, 1H), 1.15 (dddd, *J* = 14.4, 9.6, 5.6, 0.5 Hz, 1H); ^{13}C NMR (75 MHz, CD_3OD): δ 74.1, 61.4, 42.9, 40.4, 36.0, 35.8, 31.2; ^{2}H NMR (76 MHz, CH_3OH) δ 3.51 (s); HRMS (EI+) *m/z* calc'd for $C_7H_{12}O_2{}^2H_2$ $[M]^+$: 132.1119, found 132.1113. All other spectral data are consistent with reported values.

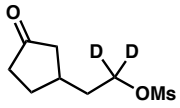

345
(65% yield, two steps)

D_2-labeled ketomesylate 345. Prepared as above to afford **345** (0.3775 g, 1.81 mmol, 65% yield over two steps) as a colorless oil. ^{1}H NMR (300 MHz, $CDCl_3$) δ 3.01 (s, 3H), 2.49–2.40 (m, 1H), 2.39–2.10 (comp m, 4H), 1.89 (d, *J* = 6.9 Hz, 2H), 1.83 (ddd, *J* = 17.5, 7.4, 1.3 Hz, 1H), 1.63–1.47 (m, 1H); ^{13}C NMR (75 MHz, $CDCl_3$) δ 218.3, 67.6 (pentet, J_{CD} = 22.7 Hz), 44.8, 38.4, 37.6, 34.7, 33.7, 29.4; ^{2}H NMR (76 MHz, $CHCl_3$) δ 4.29 (s); HRMS (EI+) *m/z* calc'd for $C_8H_{12}SO_4{}^2H_2$ $[M]^+$: 208.0738, found 208.0741. All other spectral data are consistent with reported values.

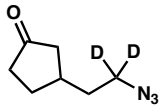

374
(97% yield)

D_2-labeled ketoazide 374. Prepared as above to afford **374** (143.6 mg, 0.925 mmol, 97% yield) as a colorless oil. ^{1}H NMR (300 MHz, $CDCl_3$) δ 2.48–2.39 (m, 1H), 2.37–2.11 (comp m, 4H), 1.83 (ddd, J = 17.6, 9.8, 1.3 Hz, 1H), 1.74 (d, J = 6.7 Hz, 2H), 1.61–1.50 (m, 1H); ^{13}C NMR (75 MHz, $CDCl_3$) δ 218.6, 49.3 (pentet, J_{CD} = 21.7 Hz), 44.8, 38.5, 34.6, 34.4, 29.4; ^{2}H NMR (76 MHz, $CHCl_3$) δ 3.32 (s). All other spectral data are consistent with reported values.

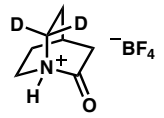

335·HBF$_4$
(27% yield)

6,6-d_2-2-quinuclidonium tetrafluoroborate (335•HBF$_4$). Prepared as above to afford **335•**HBF_4 (15.3 mg, 0.0712 mmol, 27% yield) as white needles. ^{1}H NMR (300 MHz, CD_3CN) δ 7.96 (br s, 1H), 3.77–3.58 (m, 2H), 2.97 (d, J = 3.2 Hz, 2H), 2.51 (app pentet, J = 3.2 Hz, 1H), 2.15 (m, 2H), 2.02–1.94 (m, 2H); ^{2}H NMR (76 MHz, CH_3CN) δ 3.68 (s), 3.59 (s); HRMS (FAB+) m/z calc'd for $C_7H_{10}NO^2H_2$ $[M + H]^+$: 128.1044, observed 128.1042.

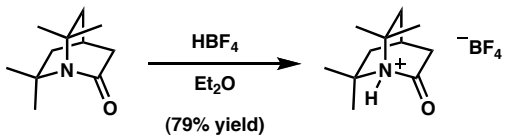

318 ***318·HBF$_4$***

6,6,7,7-tetramethyl-2-quinuclidonium tetrafluoroborate (318•HBF_4). 6,6,7,7-tetramethyl-2-quinuclidone (**318**, 24.9 mg, 0.137 mmol, 1.0 equiv) was dissolved in Et_2O (1.0 mL, 0.14 M) and HBF_4 in Et_2O (54 wt % solution, 38 μL, 0.274 mmol, 2.0 equiv) was added in one portion. The reaction was stirred for 30 min and the precipitate was collected by filtration and dried under vacuum to afford **318**•HBF_4 (31.6 mg, 0.117 mmol, 86% yield) as a tan solid. HRMS (FAB+) *m/z*) calc'd for $C_{11}H_{20}NO$ [M + H]$^+$: 182.1545, observed 182.1552.

5.6.3 COMPUTATIONALLY OPTIMIZED STRUCTURES

Bond lengths below are given in angstroms (Å). Structures were optimized at the B3LYP/6-31G* level. Total energies were then calculated at the B3LYP/6-311++G** level.

*Figure 5.6.1. Optimized structure of 2-quinuclidone (**311**).*

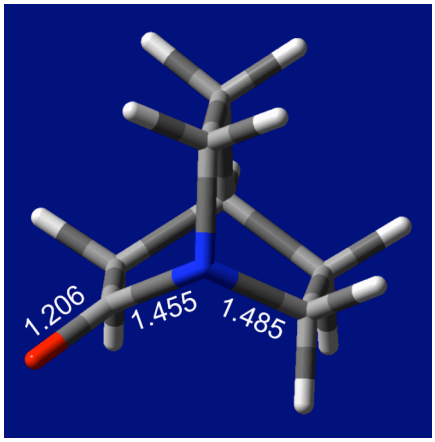

O=C–N–C dihedral angles: +121°, –121°

Total energy: –403.4361217 hartrees

*Figure 5.6.2. Optimized structure of N-protonated 2-quinuclidone (**311**•H^+).*

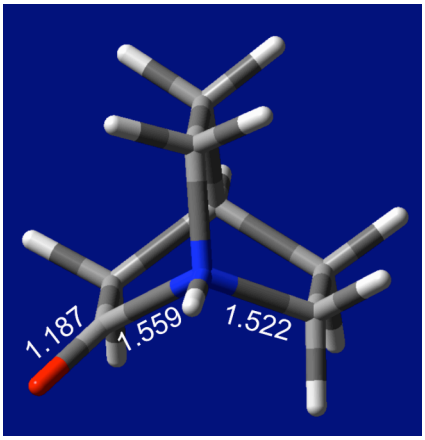

O=C–N–C dihedral angles +119°, –119°

Total energy: –403.8028617 hartrees

*Figure 5.6.3. Optimized structure of 6,6,7,7-tetramethyl-2-quinuclidone (**318**).*

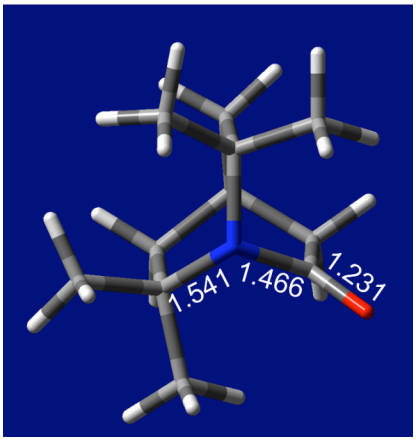

O=C–N–C dihedral angles: +118°, –118°

Total energy: –560.726844 hartrees

*Figure 5.6.4. Optimized structure of N-protonated 6,6,7,7-tetramethyl-2-quinuclidone (**318**•H^+).*

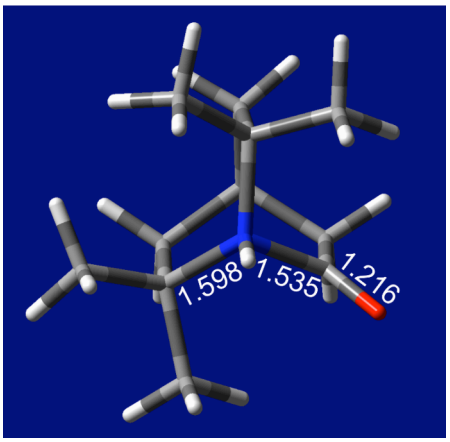

O=C–N–C dihedral angles: +116°, –116°

Total energy: –561.03524 hartrees

5.6.4 EXTENDED KINETIC METHOD PLOTS

*Figure 5.6.5. Plot of the extended kinetic method of **311** with direct entropy correction.*

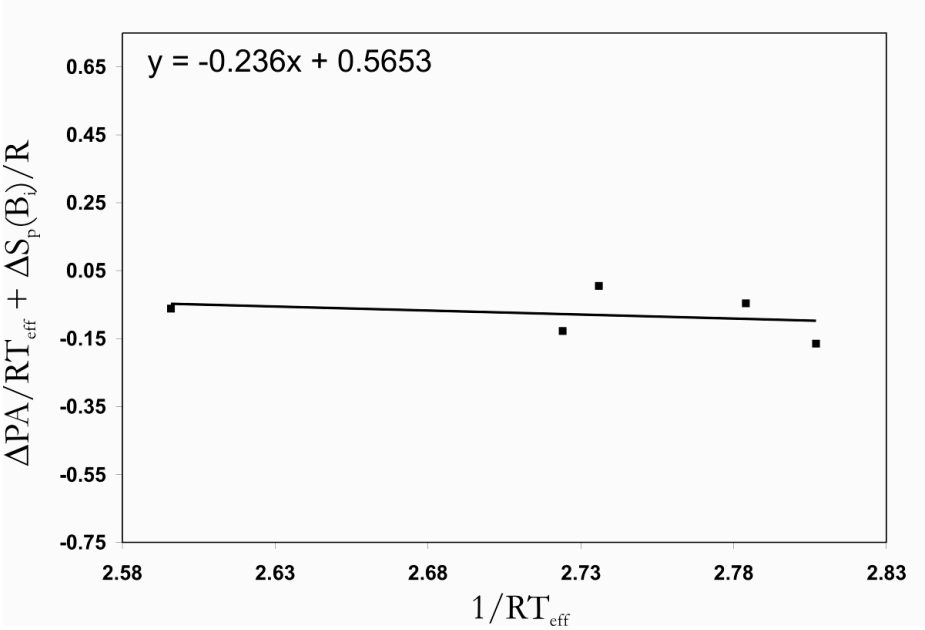

The y-intercepts from the entropy corrected kinetic method were plotted against the slopes at 18%, 25%, 35%, 50%, and 85% normalized collision energies. The slope of the line shown below is equal to [PA_{quin} – PA_{avg}].

Figure 5.6.6. Entropy corrected kinetic plot using bulky bases.

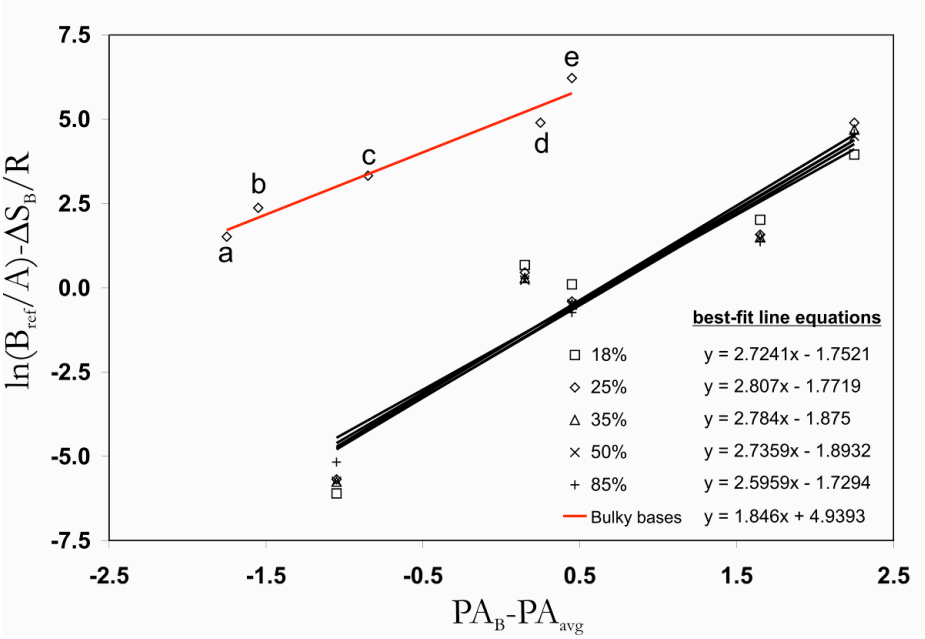

The second trend observed is associated with the proton affinity of the carbonyl oxygen of 2-quinuclidone (**311**). Bulky bases: (***a***) 3-aminopyridine; (***b***) 3,5-lutidine; (***c***) diisobutylamine; (***d***) 2,4-lutidine; (***e***) 1,4-diazabicyclo[2.2.2]-octane.

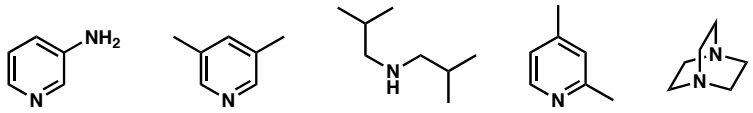

a ***b*** ***c*** ***d*** ***e***

5.6.5 MS² SPECTRA OF ISOTOPICALLY LABELED DERIVATIVES AND THEIR HYDROLYSIS PRODUCTS

Fragmentation patterns of all isotopically labeled compounds (**332**–**335**) are in agreement with mechanism proposed in Scheme 5.3.1a.

*Figure 5.6.7. MS^2 spectrum of **332** (^{15}N).*

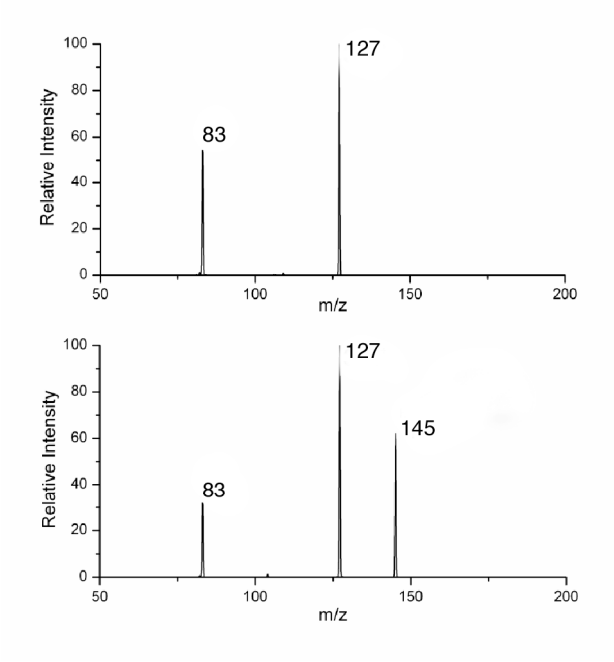

*Figure 5.6.8. MS^2 spectrum of **333** ($^{13}C_2$).*

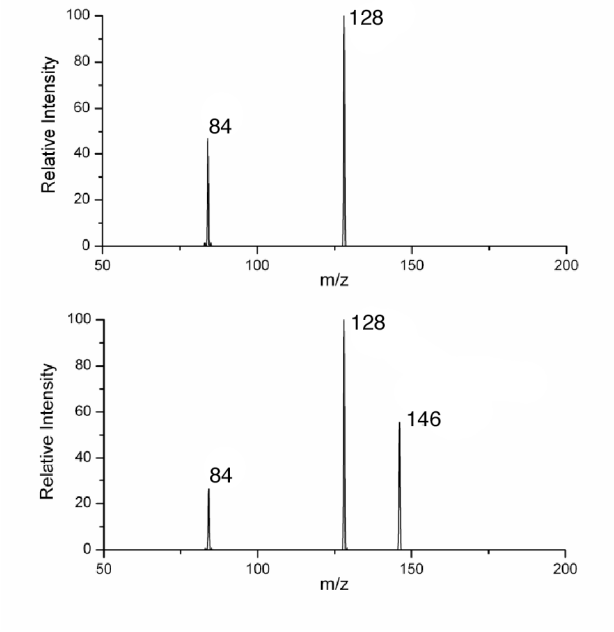

*Figure 5.6.9. MS^2 spectrum of **334** (D).*

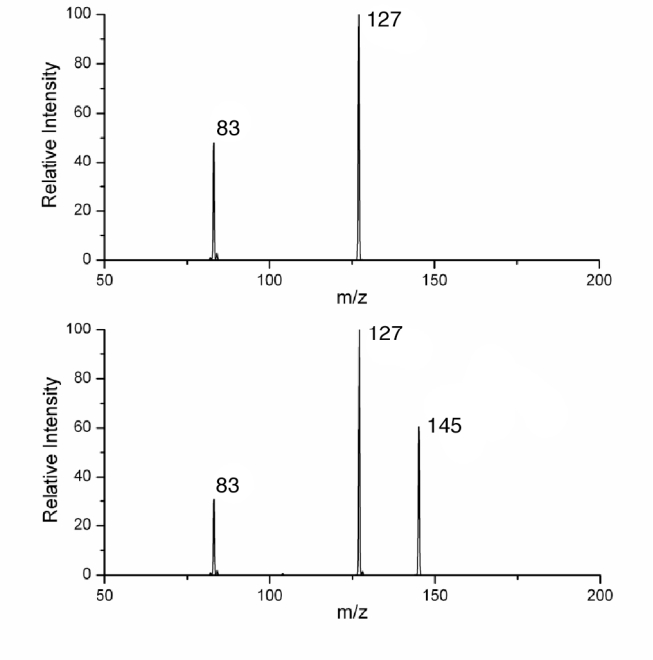

*Figure 5.6.10. MS^2 spectrum of **335** (D_2).*

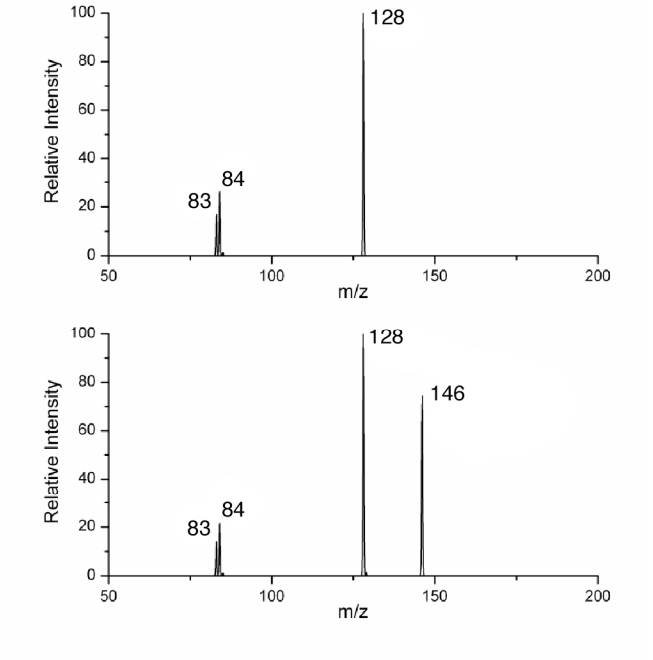

5.7 NOTES AND REFERENCES

(1) Greenberg, A., Breneman, C. M., Liebman, J. F., Eds. *The Amide Linkage: Selected Structural Aspects in Chemistry, Biochemistry, and Materials Science;* Wiley: New York, 2000.

(2) Smith, R. M.; Hansen, D. E. *J. Am. Chem. Soc.* **1998**, *120*, 8910–8913.

(3) (a) Wiberg, K. B. *Acc. Chem. Res.* **1999**, *32*, 922–929. (b) Kemnitz, C. R.; Loewen, M. J. *J. Am. Chem. Soc.* **2007**, *129*, 2521–2528.

(4) (a) Greenberg, A.; Venanzi, C. A. *J. Am. Chem. Soc.* **1993**, *115*, 6951–6957. (b) Greenberg, A.; Moore, D. T.; DuBois, T. D. *J. Am. Chem. Soc.* **1996**, *118*, 8658–8668.

(5) Greenberg, A. Twisted Bridgehead Bicyclic Lactams. In *Structure and Reactivity;* Liebman, J. F., Greenberg, A., Eds.; VCH: New York, 1988; pp 139–178.

(6) (a) Bennet, A. J.; Wang, Q.-P.; Slebocka-Tilk, H.; Somayaji, V.; Brown, R. S.; Santarsiero, B. D. *J. Am. Chem. Soc.* **1990**, *112*, 6383–6385. (b) Ballester, P.; Tadayoni, B. M.; Branda, N.; Rebek, J., Jr. *J. Am. Chem. Soc.* **1990**, *112*, 3685–3686. (c) Kirby, A. J.; Komarov, I. V.; Feeder, N. *J. Am. Chem. Soc.* **1998**, *120*, 7101–7102. (d) Lopez, X.; Mujika, J. I.; Blackburn, G. M.; Karplus, M. *J. Phys. Chem. A* **2003**, *107*, 2304–2315. (e) Mujika, J. I.; Mercero, J. M.; Lopez, X. *J. Am. Chem. Soc.* **2005**, *127*, 4445–4453.

(7) (a) Poland, B. W.; Xu, M.-Q.; Quiocho, F. A. *J. Biol. Chem.* **2000**, *275*, 16408–16413. (b) Romanelli, A.; Shekhtman, A.; Cowburn, D.; Muir, T. W. *Proc. Natl. Acad. Sci. U.S.A.* **2004**, *101*, 6397–6402. (c) Johansson, D. G. A.; Wallin, G.;

Sandber, A.; Macao, B.; Åqvist, J.; Härd, T. *J. Am. Chem. Soc.* **2009**, *131*, 9475–9477.

(8) For reviews of the *cis–trans* isomerization of peptides, see: (a) Wawra, S.; Fischer, G. Amide *Cis–Trans* Isomerization in Peptides and Proteins. In *cis–trans Isomerization in Biochemistry;* Dugave, C., Ed.; Wiley-VCH: Weinheim, 2006; pp 167–193. (b) Fischer, G. Enyzmes Catalyzing Peptide Bond *Cis–Trans* Isomerizations. In *cis–trans Isomerization in Biochemistry;* Dugave, C., Ed.; Wiley-VCH: Weinheim, 2006; pp 195–224. (c) Dugave, C.; Demange, L. *Chem. Rev.* **2003**, *103*, 2475–2532.

(9) Lukeš, R. *Coll. Czech. Chem. Commun.* **1938**, *10*, 148–152.

(10) Bredt, J. *Liebigs Ann. Chem.* **1924**, *437*, 1–13.

(11) (a) Johnson, J. R.; Woodward, R. B.; Robinson, R. The Constitution of the Penicillins. *The Chemistry of Penicillin;* Clark, H. T., Johnson, J. R., Robinson, R., Eds.; Princeton University Press: Princeton, NJ, 1949; pp 440–454. (b) Wasserman, H. H. *Heterocycles* **1977**, *7*, 1–15. (c) Wasserman, H.H. *Nature* **2006**, *441*, 699–700.

(12) Yakhontov, L. N.; Rubsitov, M. V. *J. Gen. Chem. USSR* **1957**, *27*, 83–87.

(13) Pracejus, H.; Kehlen, M.; Matschiner, H. *Tetrahedron* **1965**, *21*, 2257–2270.

(14) (a) Pracejus, H. *Chem. Ber.* **1959**, *92*, 988–998. (b) Pracejus, H. *Chem. Ber.* **1965**, *98*, 2897–2905. (c) Levkoeva, E. I.; Nikitskaya, E. S.; Yakhontov, L. N. *Dokl. Akad. Nauk SSSR* **1970**, *192*, 342–345. (d) Greenberg, A.; Wu, G.; Tsai, J.-C.; Chiu, Y.-Y. *Struct. Chem.* **1993**, *4*, 127–129.

(15) (a) Hall, H. K.; Shaw, R. G.; Deutschmann, A. *J. Org. Chem.* **1980**, *45*, 3722–3724. (b) Blackburn, G. M.; Skaife, C. J.; Kay, I. T. *J. Chem. Res., Miniprint* **1980**, 3650–3669. (c) Buchanan, G. L.; Kitson, D. H.; Mallinson, P. R.; Sim, G. A.; White, D. N. J.; Cox, P. J. *J. Chem. Soc., Perkin Trans. 2* **1983**, 1709–1712. (d) Somayaji, V.; Brown, R. S. *J. Org. Chem.* **1986**, *51*, 2676–2686. (e) Williams, R. M.; Lee, B. H. *J. Am. Chem. Soc.* **1986**, *108*, 6431–6433. (f) Williams, R. M.; Lee, B. Y.; Miller, M. M.; Anderson, O. P. *J. Am. Chem. Soc.* **1989**, *111*, 1073–1081. (g) Wang, Q.-P.; Bennet, A. J.; Brown, R. S.; Santarsiero, B. D. *Can. J. Chem.* **1990**, *68*, 1732–1739. (h) Boivin, J.; Gaudin, D.; Labrecque, D.; Jankowski, K. *Tetrahedron Lett.* **1990**, *31*, 2281–2282. (i) Wang, Q.-P.; Bennet, A. J.; Brown, R. S.; Santarsiero, B. D. *J. Am. Chem. Soc.* **1991**, *113*, 5757–5765. (j) Lease, T. G.; Shea, K. J. *J. Am. Chem. Soc.* **1993**, *115*, 2248–2260. (k) Kirby, A. J.; Komarov, I. V.; Wothers, P. D.; Feeder, N. *Angew. Chem., Int. Ed.* **1998**, *37*, 785–786. (l) Bashore, C. G.; Samardjiev, I. J.; Bordner, J.; Coe, J. W. *J. Am. Chem. Soc.* **2003**, *125*, 3268–3272. (m) Ribelin, T. P.; Judd, A. S.; Akritopoulou-Zanze, I.; Henry, R. F.; Cross, J. L.; Whittern, D. N.; Djuric, S. W. *Org. Lett.* **2007**, *9*, 5119–5122. (n) Szostak, M.; Aube, J. *Org. Lett.* **2009**, *11*, 3878–3881.

(16) Mujika, J. I.; Mercero, J. M.; Lopez, X. *J. Phys. Chem. A* **2003**, *107*, 6099–6107.

(17) Clayden, J.; Moran, W. J. *Angew. Chem., Int. Ed.* **2006**, *45*, 7118–7120.

(18) Tani, K.; Stoltz, B. M. *Nature* **2006**, *441*, 731–734.

(19) A separate C–H activation approach was pursued incorporating the loss of dinitrogen. However, neither **311** nor any products consistent with its decomposition were observed.

(20) Aubé, J.; Milligan, G. L. *J. Am. Chem. Soc.* **1991**, *113*, 8965–8966.

(21) (a) Golden, J. E.; Aubé, J. *Angew. Chem., Int. Ed.* **2002**, *41*, 4316–4318. (b) Lei, Y.; Wrobleski, A. D.; Golden, J. E.; Powell, D. R.; Aubé, J. *J. Am. Chem. Soc.* **2005**, *127*, 4552–4553. (c) Yao, L.; Aubé, J. *J. Am. Chem. Soc.* **2007**, *129*, 2766–2767.

(22) The ratio of **311**:**326** was determined by exposure to MeOH and analysis of the ring-opened products.

(23) Pretsch, E.; Bühlmann, P.; Affolter, C. *Structure Determination of Organic Compounds. Tables of Spectral Data,* 3rd ed.; Springer-Verlag: New York, 2000.

(24) Dunitz, J. D.; Winkler, F. K. *Acta Crystallogr., Sect. B: Struct. Sci.* **1975**, *31*, 251–263.

(25) Wiberg, K. B.; Laidig, K. E. *J. Am. Chem. Soc.* **1987**, *109*, 5935–5943.

(26) (a) Zheng, X.; Cooks, R. G. *J. Phys. Chem. A* **2002**, *106*, 9939–9946. (b) Bouchoux, G.; Sablier, M.; Berruyer-Penaud, F. *J. Mass Spectrom.* **2004**, *39*, 986–997.

(27) (a) Wu, Z.; Fenselau, C.; Cooks, G. R. *Rapid Commun. Mass. Spectrom.* **1994**, *8*, 777–780. (b) Cerda, B. A.; Wesdemiotis, C. *J. Am. Chem. Soc.* **1995**, *117*, 9734–9739. (c) Armentrout, P. B. *J. Am. Soc. Mass Spectrom.* **2000**, *11*, 371–379.

(28) Hunter, E. P.; Lias, S. G. Proton Affinity Evaluation. In *NIST Chemistry WebBook, NIST Standard Reference Database Number 69*, Linstrom, P. J., Mallard, W. G., Eds.; National Institute of Standards and Technology, Gaithersburg, MD, 2005; 20899 (http://webbook.nist.gov).

(29) Previous calculations have determined a 22.8 kcal/mol difference in energy for the site of protonation of **311**. See ref 4b.

(30) See subsection 5.6.4 for details.

(31) Hunter, E. P.; Lias, S. G.; *J. Phys. Chem. Ref. Data* **1998**, *27*, 413–656.

(32) (a) McLafferty, F. W. *Anal. Chem.* **1956**, *28*, 306–316. (b) Kingston, D. G. I.; Bursey, J. T.; Bursey, M. M. *Chem. Rev.* **1974**, *74*, 215–242.

(33) (a) Tomioka, H.; Oshima, K.; Nozaki, H. *Tetrahedron Lett.* **1982**, *23*, 539–542. (b) Kanemoto, S.; Tomioka, H.; Oshima, K.; Nozaki, H. *Bull. Chem. Soc. Jpn.* **1986**, *59*, 105–108.

(34) (a) Gannon, W. F.; House, H. O. *Org. Synth.* **1973**, *CV 5*, 294–196. (b) Dauphin, G.; Gramain, J.-C.; Kergomard, A.; Renard, M. F.; Veschambre, H. *J. Chem. Soc., Chem. Commun.* **1980**, 318–319.

(35) See subsection 5.6.5 for details.

(36) Westheimer, F. H. *Chem. Rev.* **1961**, *61*, 265–273.

(37) Wiberg, K. B. *Angew., Int. Ed. Engl.* **1986**, *25*, 312–322.

(38) The parent bicyclic amines **375** and **376** possess a similar pK_a values (10.90 and 10.53, respectively), however their nucleophilic reactivities are significantly different with **375** as the stronger nucleophile. See: Hine, J.; Chen, Y.-J. *J. Org. Chem.* **1987**, *52*, 2091–2094.

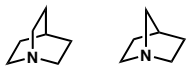

375 ***376***

(39) Danheiser, R. L.; Savariar, S.; Cha, D. D. *Organic Syntheses;* Wiley & Sons: New York, 1993; Collect. Vol. VIII, pp 82–86.

(40) Qin, D.-G.; Zha, H.-Y.; Yao, Z.-H. *J. Org. Chem.* **2002**, *67*, 1038–1040.

(41) This cyclization has been used for substituted cyclobutanone systems. See ref 20.

(42) (a) Coll, J. C.; Crist, D. R.; Barrio, M. G.; Leonard, N. J. *J. Am. Chem. Soc.* **1972**, *94*, 7092–7099. (b) Wang, A. H.-J.; Missavage, R. J.; Byrn, S. R.; Paul, I. C. *J. Am. Chem. Soc.* **1972**, *94*, 7100–7104.

(43) (a) Maier, W. F.; Schleyer, P. v. R. *J. Am. Chem. Soc.* **1981**, *103*, 1891–1900. (b) McEwen, A. B.; Schleyer, P. v .R. *J. Am. Chem. Soc.* **1986**, *108*, 3951–3960.

(44) Schomaker, J. M.; Pulgam, V. R.; Borhan, B. *J. Am. Chem. Soc.* **2004**, *126*, 13600–13601.

(45) Gottlieb, H. E.; Kotlyar, V.; Nudelman, A. *J. Org. Chem.* **1997**, *62*, 7512–7515.

(46) Andersson, M. P.; Uvdal, P. *J. Phys. Chem. A* **2005**, *109*, 2937–2941.

(47) Boys, S. F.; Bernardi, F. *Mol. Phys.* **1970**, *19*, 553–566.